



Diurnal variations of rainfall affected by complex topography based on high-density observation in Chongqing over southwest China

Qiang Li¹ · Yongguang Zheng² · Guobing Zhou¹ · Yan Zhu¹ · Chao Liu¹ · Yan Liu³

Received: 5 August 2021 / Accepted: 27 December 2021 / Published online: 15 March 2022
© The Author(s) 2022

Abstract

Located in the eastern edge of the Sichuan Basin (SCB) in the southwest China, Chongqing is a mountainous region with typical complex topographic features. Using the hourly rainfall observation data of high-density 1686 meteorological stations in Chongqing during warm season from 2009 to 2016, we investigated the diurnal characteristics of precipitation affected by complex topography. The complex mountainous terrain has a significant impact on diurnal variations and distinct regional features of rainfall amount, frequency, and intensity. The stations located in the higher complex mountainous areas have greater rainfall amount, frequency, and intensity than those in the lower surrounding areas. In addition, the detailed characteristics of the rainfall amount and frequency in the four study regions further show that the rainfall amount and frequency significantly increase with the rise of elevation, especially in the area that terrain height sharply increases along the mountain extending direction. The diurnal variation of the rainfall amount is characterized by a bimodal structure with a dominant early-morning peak occurring at approximately 0700 LST (23 UTC) and a weaker secondary late-afternoon peak at approximately 1600 LST (08 UTC), while the rainfall frequency has a single early-morning peak. The terrain height has a significant impact on the proportions of the early-morning rainfall. With the elevation increasing in the four study regions, the proportions of rainfall amount (frequency) that occurs during early-morning period decrease.

1 Introduction

The complex topography plays a significant role in the inhomogeneous spatial and temporal distributions of rainfall patterns, and most previous researches have shown that the mechanisms of the orographic influences are complex (Smith 1979; Jiang and Smith 2003; Colle 2004; Smith and Barstad 2004; Roe 2005; Rotunno and Houze 2007; Kirshbaum 2011; Houze 2012; Couto et al. 2016; DeHart and Houze 2017; Purnell and Kirshbaum 2018; Kang et al. 2019). Many features of mountainous topography, including elevation, relief amplitude, slope, and aspect, can initiate, enhance,

and modify rainfall and further influence diurnal and spatial variations of rainfall (Weisse and Bois 2001; Burbank et al. 2003; Lee et al. 2010; Chen et al. 2013; White and Paul 2015; Kirshbaum et al. 2018; Sarmadi et al. 2019). Among the orographic and morphological characteristics, elevation differences perform a considerable important function in the spatial variation of climatic rainfall in mountainous regions (Basist et al. 1994; Goovaerts 2000; Johansson and Chen 2003; Sokol and Bližňák 2009; Silverman et al. 2013).

The topography in China has complex and various with diverse mountain ranges and plateaus; therefore, the influence of terrain on precipitation is more complex (Tao 1980; Peng et al. 1995; Liao et al. 2007; Yu et al. 2014). Due to the forcing effects of spatial scale and height differences of complex topography, the spatiotemporal characteristics of precipitation demonstrate fairly obvious regional differences (Wang et al. 2013; Li et al. 2017, 2019, 2020a, b; Yu et al. 2018). The influences on rainfall in the high Tibetan Plateau (TP) region are not only closely related to the spatiotemporal distributions of rainfall in the local and the surrounding areas (Liu et al. 2009; Xu and Zipser 2011; Jin et al. 2013; Guo et al. 2014, 2016; Cuo and Zhang 2017; Li 2017; Chen et al. 2018), but also to diurnal variations of rainfall in the faraway

✉ Guobing Zhou
zhou-gb@163.com

Qiang Li
cqlqlq@163.com

¹ Chongqing Meteorological Observatory, 68 Xinpaifang First Rd., Yubei District, Chongqing 410047, China

² National Meteorological Centre, Beijing 100081, China

³ State Grid Chongqing Electric Power Company, Chongqing 410015, China

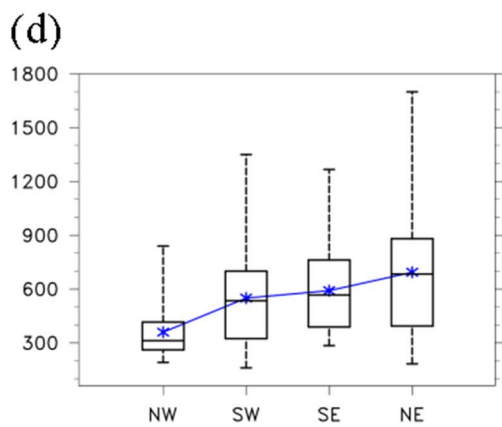
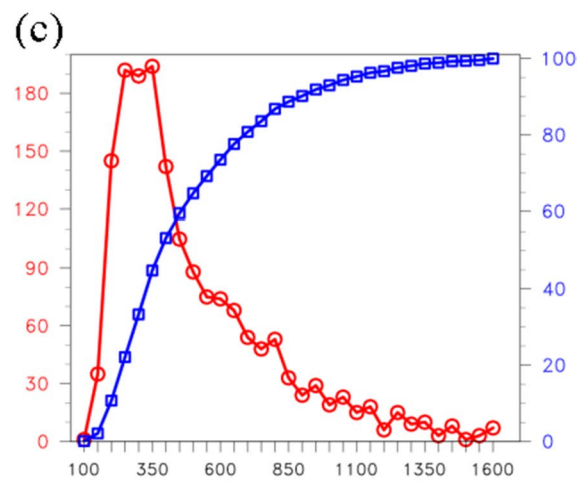
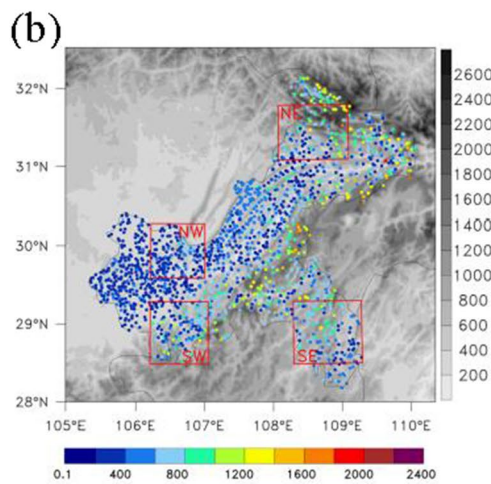
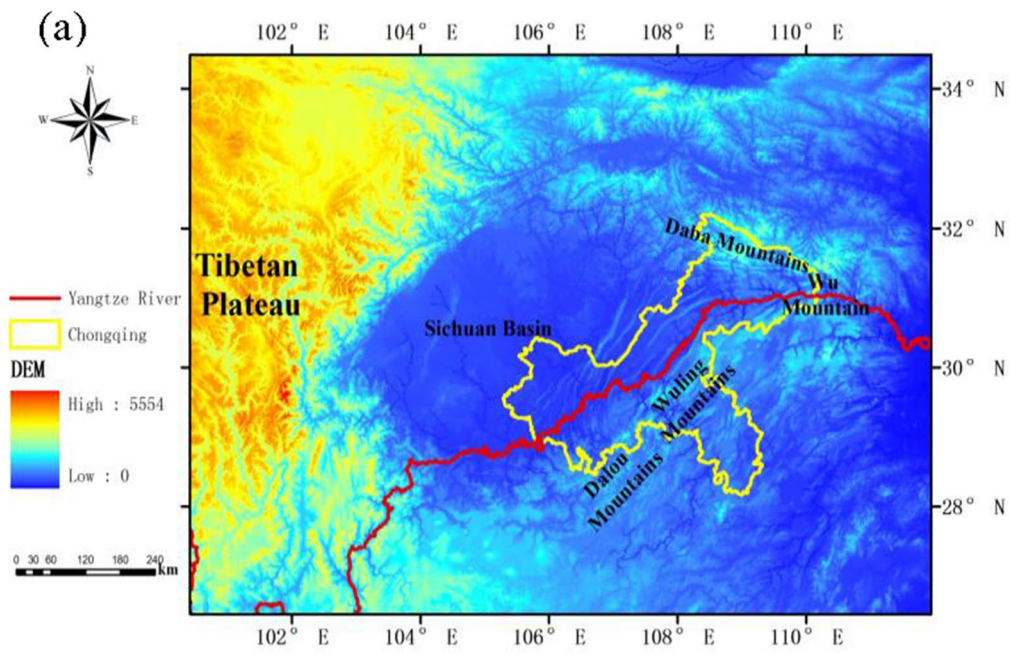


Fig. 1 a the geographical location of Chongqing (yellow lines). The red line shows the Yangtze River. The distributions of 1868 rain gauge stations (b: colored dots). The red boxes represent four study areas. Gray shadings indicate topography (unit: m). The numbers of station (c: left y-axis) as a function of terrain height (c: x-axis, the 1600 m scale of x-axis indicates the numbers of stations above 1600 m) (c) and the proportions of different terrain height (c: right y-axis). Boxplot of stations terrain height of the four study regions (d); box shows lower and upper quartiles. Black lines inside boxes represent medians. Blue dots are for average terrain elevation. Minimum and maximum values are shown by whiskers. NW, SW, SE and NE indicate the northwestern study area, the southwestern study area, the southeastern study area, and the northeastern study area respectively, and the same meaning is shown in the following figure

east in China (Bao et al. 2011; Zhang et al. 2014a, b; Wang et al. 2018). However, regional topography only force local circulations that affect the local features of diurnal variation (Barros and Lang 2003; Chen et al. 2013; Li et al. 2017). Yuan et al. (2014) found the spatiotemporal features of rainfall events were highly correlated with elevation heights over North China and the topography influenced the diurnal varied surface or low-level temperature, moisture, and wind fields. The locally enhanced convergence in the Dabie Mountains provides the strongest thermal and dynamic forcing lifting that initiates the earliest convective cells, which leads to condensation and formation of the morning precipitation peak (Wang et al. 2016; Fu et al. 2019). Li et al. (2019) revealed the influences of the gauge elevations on the diurnal variation of rainfall, and the proportion of the rainfall frequency occurring during the early-morning period decreases with increasing elevations over the Qilian Mountains. Gan et al. (2019) proposed that typical small-scale Mount Tai exhibits great differences in precipitation characteristics with a large enhancement effect on rainfall, which was different from the surrounding areas. When precipitation of Mount Tai is significantly enhanced, the corresponding wind field tends to be dominated by stronger southwesterly. These studies show that the isolated mountainous topography plays a crucial role in spatial and temporal variation of precipitation. However, the details about the spatial variation of precipitation over complex topography are not consistent, especially for the possible links between mountainous features and precipitation over different areas of complex topography.

In recent years, with the appearance of multi-year continuous hourly rainfall data, an increasing number of studies have focused on the diurnal cycles of the rainfall characteristics in many regions around the world (Leahy and Kiely 2011; Deshpande et al. 2012; Hitchens et al. 2013; Stevenson and Schumacher 2014; Iwasaki 2012 2015). Similar researches on diurnal variations of precipitation based on hourly rainfall data have also made great progress over mainland China (Yu et al. 2007a, b, 2014; Chen et al. 2015; Liang and Ding 2017; Li et al. 2017). Using a long-term dataset comprising measurements made at more than 2420 stations

over SCB, Zheng et al. (2016) found that the SCB experienced higher rainfall accumulations and a higher occurrence of short-duration heavy rainfall events compared with other sub-regions of China. Based on the same datasets, Luo et al. (2016) reported that extreme hourly rainfall over SCB peaks in July. Furthermore, based on daily precipitation data from 524 observation stations, Zhang et al. (2019a) revealed that, on the regional scale, some differences existed in the changes of autumn rainfall between the eastern and the western parts of West China. In addition, based on hourly rainfall data of 468 rain gauge stations, Chen et al. (2021) studied spatial and temporal characteristics of abrupt heavy rainfall events (AHRE) over southwest China, and the occurrence frequency of these AHRE exhibited large spatial variability among different regions. Nevertheless, the previous studies used observations at the limited automatic meteorological stations and lacked precipitation data with a higher spatial resolution; their results show some regional differences on precipitation diurnal variations over China. Due to the sparse gauge networks and the large spatial and temporal variations of rainfall, obtaining accurate finding has been challenging for scientists especially in complex terrain.

Located close to the eastern edge of SCB in the southwest China (Fig. 1a), Chongqing ($105^{\circ} 11' \sim 110^{\circ} 11' \text{ E}$, $28^{\circ} 10' \sim 32^{\circ} 13' \text{ N}$) is a mountainous region in the middle and upper reaches of the Yangtze River and has a humid subtropical monsoon climate zone affected by the TP significantly. Chongqing, known as “mountain city”, has special geographical conditions with relatively flat terrain in the Sichuan Basin and mountains along the edge of the basin. Recently, considerable studies have been conducted to reveal the effects of orography on diurnal variation of nocturnal precipitation peak time over SCB (Zhang et al. 2014a; Chen et al. 2017; Xue et al. 2018). In addition, the movement of precipitation over the SCB and the adjacent regions is closely tied to multiple regional-scale mountain-plain sole-noids because of the great contrast in terrain heights between the SCB and surrounding mountain ranges (Qian et al. 2015). Zhang et al. (2019b) demonstrated that prominent diurnal inertial oscillations of south-southwesterly low-level jet into the southeast side of the SCB played an important role in modulating the diurnal variation of precipitation over the SCB. Li et al. (2020a, b) found there is a prominent northeastward time delay of precipitation peak over the SCB, and the diurnal variation of 850 hPa wind has strong easterly wind deviations in the early evening, which favors for an initiation of precipitation by orographic lift of air. However, few studies have reported on the rainfall diurnal cycle in Chongqing, especially achievement between rainfall and terrain. Using the hourly precipitation data observed at 34 gauge stations in Chongqing, Chen et al. (2019) revealed the spatial and temporal characteristics of the precipitation. By selecting 16 representative stations in two types of terrain

for analysis, the results showed that the amplitude of diurnal precipitation at the stations in higher terrain was smaller. The studies yielded somewhat significant results in this area. Nevertheless, derived from rare stations, studies cannot be conducted to analyze the detailed characteristics of rainfall over the complex topography in Chongqing. Hence, more thorough researches need to be carried out on the diurnal variation of precipitation based on hourly precipitation observed from automatic meteorological stations and high-density regional meteorological stations.

In this study, based on high-density and quality-controlled hourly rain gauge data, detailed spatiotemporal characteristics of rainfall amount, frequency, intensity, and durations in the different topographic areas over Chongqing are investigated. In addition, the relationships between the diurnal characteristics and the complex topography will also be revealed. The structure of this paper is organized as follows. Section 2 describes study region, the datasets and analysis methods. Section 3 shows the detailed spatial–temporal distributions features of rainfall, the detailed characteristics of diurnal evolution, and the relations between early-morning rainfall and the elevation. Finally, conclusion and discussion is given in Section 4.

2 Study region, data, and methods

2.1 Description of the study area

Chongqing has one of the most typical complex topographic features located in an inland area, which is the transitional region between the second and third topographical steps of China (Fig. 1a). The west Chongqing goes deep into the SCB at low elevation, while the east Chongqing gradually rises eastward with high terrain spreading on the Wu Mountain (WM) and reaches the middle of the Yangtze River. The south Chongqing is adjacent to the Dalou Mountains (DLM) and the Wuling Mountains (WLM), and the north Chongqing lays back the Daba Mountains (DBM). The topography inclines from the west toward the Yangtze River valley and can be divided into the following categories: plains, hills, mid-height mountains, and tablelands. The mountains, hills, tablelands, and plains account for 75.9%, 17.0%, 3.57%, and 2.39%, respectively, of the total land area (Chongqing Bureau of Geology and Minerals Exploration (CBGM) 2002).

Figure 1c shows numbers of station at different terrain heights. Initially, the numbers rapidly increase from 100 to 250 m with maximum value reaching between 200 and 500 m (62.6% of all stations) and then gradually reduce from 500 to 1600 m. The proportions of stations below 500 and below 1000 m to total stations are 64.7% and 93.0%, respectively.

Because of the complex terrain, in order to illustrate the detailed features of rainfall and to facilitate further obtaining links between mountainous features and rainfall over different areas in Chongqing, we select four typical areas by considering the topographical features, as shown by red boxes in Fig. 1b. The northwestern study area (NW) denotes the complex topography of mixed basin and hills, and the southwestern study area (SW) is the mountainous terrain in southwest Chongqing adjacent to the northern DLM. The southeastern study area (SE) represents mountainous terrain in southeast Chongqing, and the northeastern study area (NE) is mountainous terrain in northeast in which the DBM lays. The numbers of stations in NW, SW, SE, and NE are 149, 145, 111, and 141 stations, respectively. The statistics of station heights in every area are shown in Fig. 1d. The average elevation gradually increases from 359.7 m in the NW to 693.8 m in the NE. Meanwhile, the lower quartile, median, and upper quartile values of terrain height also increase, ranging from 261, 312.3, and 416 m, respectively, in the NW, to 394, 683.9, and 881 m in the NE, respectively. In addition, for each area in Fig. 1d, the minimum height is relatively consistent, and the maximum is relatively high, which is above 1000 m in the SW (1350 m), SE (1267 m), and NE (1723 m), respectively. This altitude difference is mainly due to the difference in the variation of the underlying surface on complex terrain, especially in the SW and NE.

2.2 Station data and data processing

The hourly rain gauge observations data were obtained from the National Meteorological Information Centre (NMIC) of the China Meteorological Administration, which includes a total of 1686 surface automatic weather stations (Fig. 1b) and covers the entire warm season (May–September) from 2016 to 2020 in Chongqing. This dataset has undergone a series of strict quality control, including extreme value check, internal consistency check, and a time consistency check (CMA 2003). The information of this data set can be obtained from <http://www.cma.gov.cn/2011qx/fw/2011q/sjgx/>. To minimize the impact of missing values on the analysis, for the hourly precipitation data, the missing data must be less than 1% of the total records for 5 years series, and every station has more than 17,370 h without missing or suspicious values. Although the reconstruction is necessary for guaranteeing the completeness of the dataset and for raising the statistical confidence, we find that there is little difference between the analysis results through a comparison of the reconstructed and unreconstructed data.

2.3 Methods

In this study, following the previous studies (Dai et al. 1999; Liang et al. 2004; Yu et al. 2007a, b; Zhou et al.

2008), the definitions of the four rainfall features in this study are depicted as follows.

- (1) Rainfall amount: cumulative amount with measurable rainfall (rainfall rate $\geq 0.1 \text{ mm h}^{-1}$) divided by the number of non-missing hours during the study period.

$$\text{Rainfall amount} = P_r / N_{nm}$$

P_r is the accumulated rainfall amount with measurable rainfall during the study period; N_{nm} is the number of hours with no missing rainfall records.

- (2) Rainfall frequency: cumulative total hours with measurable rainfall (rainfall rate $\geq 0.1 \text{ mm h}^{-1}$) divided by the number of non-missing hours during the study period.

$$\text{Rainfall frequency} = N_r / N_{nm}$$

N_r is the number of hours with measurable rainfall.

- (3) Rainfall intensity: cumulative rainfall divided by the number of rainy hours during the study period.

$$\text{Rainfall intensity} = P_r / N_r$$

- (4) Rainfall event: According to the definition of previous precipitation events, we define rainfall a single rainfall event by their durations without any intermittence or at most 1-h intermittence. When a rainfall event begins and its intermittence lasts for 2 h, we deem that the rainfall after the intermittence belongs to a new rainfall event. The starting time of a rainfall event is defined as the time no rainfall in the previous 2 or more than 2 h before measurable rainfall event ($\geq 0.1 \text{ mm/h}$) occurs. The ending of a rainfall event is defined as the time there is no rainfall in the next two or more than 2 h after measurable rainfall event ($\geq 0.1 \text{ mm/h}$) occurs. The numbers of rainfall events are defined as the accumulated numbers of the total rainfall events during the whole warm season precipitation period. The duration time (rainfall amount) is defined as the hours (accumulated rainfall amount) from the starting time to the ending time during a rainfall event, during which the intermittence is less than 1 h. The most frequent starting time of rainfall events is considered as the time when rainfall events occur most frequently, and the most frequent peaking and ending time are similarly defined.

For each type of rainfall events, let $R_a(h)$ represent the amount of hourly rainfall at time h . The normalized diurnal variation of precipitation, $D_a(h)$, is calculated by:

$$D_a(h) = \left(\frac{R_a(h)}{\frac{1}{24} \sum_{i=1}^{24} R_a(i)} - 1 \right)$$

The $R_a(h)$ is resulted from an average of the rainfall events with a specific duration. Since warm season rainfall is the main flood season and accounts for more than 85% of the annual rainfall in Chongqing (Liu et al. 2012), this study focuses on warm season.

3 Results

3.1 Spatial characteristics of warm season rainfall in Chongqing

The spatial distributions of warm season rainfall amount, frequency, and intensity in Chongqing are shown in Fig. 2, which have distinct differences for stations with different gauge elevations. As illustrated in Fig. 2a, the spatial distributions of the rainfall amount are apparently inhomogeneous. The average rainfall amount at elevations below 500 m, between 500 and 1000 m, and above 1000 m is 0.21 mm/h, 0.23 mm/h, and 0.25 mm/h, respectively. Large rainfall amount value, i.e., those above 0.21 mm/h, occur in the northern sections of DLM, the southern sections of DBM, the southern sections of WLM, and mountainous areas in the southeast Chongqing. On the contrary, small value stations of rainfall amount are located in most of the central and the western regions, and the eastern and southern sections of the northeast Chongqing. It should not be ignored that scattered stations of large rainfall amount values locate in Huarong Mountain in the NW.

The distribution patterns of frequency (Fig. 2b) are consistent with the rainfall amount. The average rainfall frequency of below 500 m, between 500 and 1000 m, and above 1000 m is 0.13, 0.14, and 0.17, respectively. The ratios of stations rainfall amount exceeding 0.21 mm/h (89%) and frequencies exceeding 0.13 (94%) above 1000 m are approximately twice more than those below 500 m (44%, 46%). The ratios are 72% and 79% between 500 and 1000 m. In other words, it is clear that the rainfall amount and frequency over mountainous areas are much higher than that in surrounding low elevation areas.

The distribution of intensity (Fig. 2c) is slightly different from the previous two with the intensity below 500 m, between 500 and 1000 m, and above 1000 m are 1.62, 1.63, and 1.55 mm/h, respectively. The proportions of intensity exceeding 1.55 mm/h are 63%, 64%, and 45%, respectively. Large values appear in the northern sections DLM, the southern sections of DBM, mountainous areas in southeast, and hilly areas in NW. It can still be found that stations with large rainfall intensity value scatter in Huarong Mountain. Compared with rainfall amount and frequency large values, the distributions of large rainfall intensity values are not entirely coincident, which do

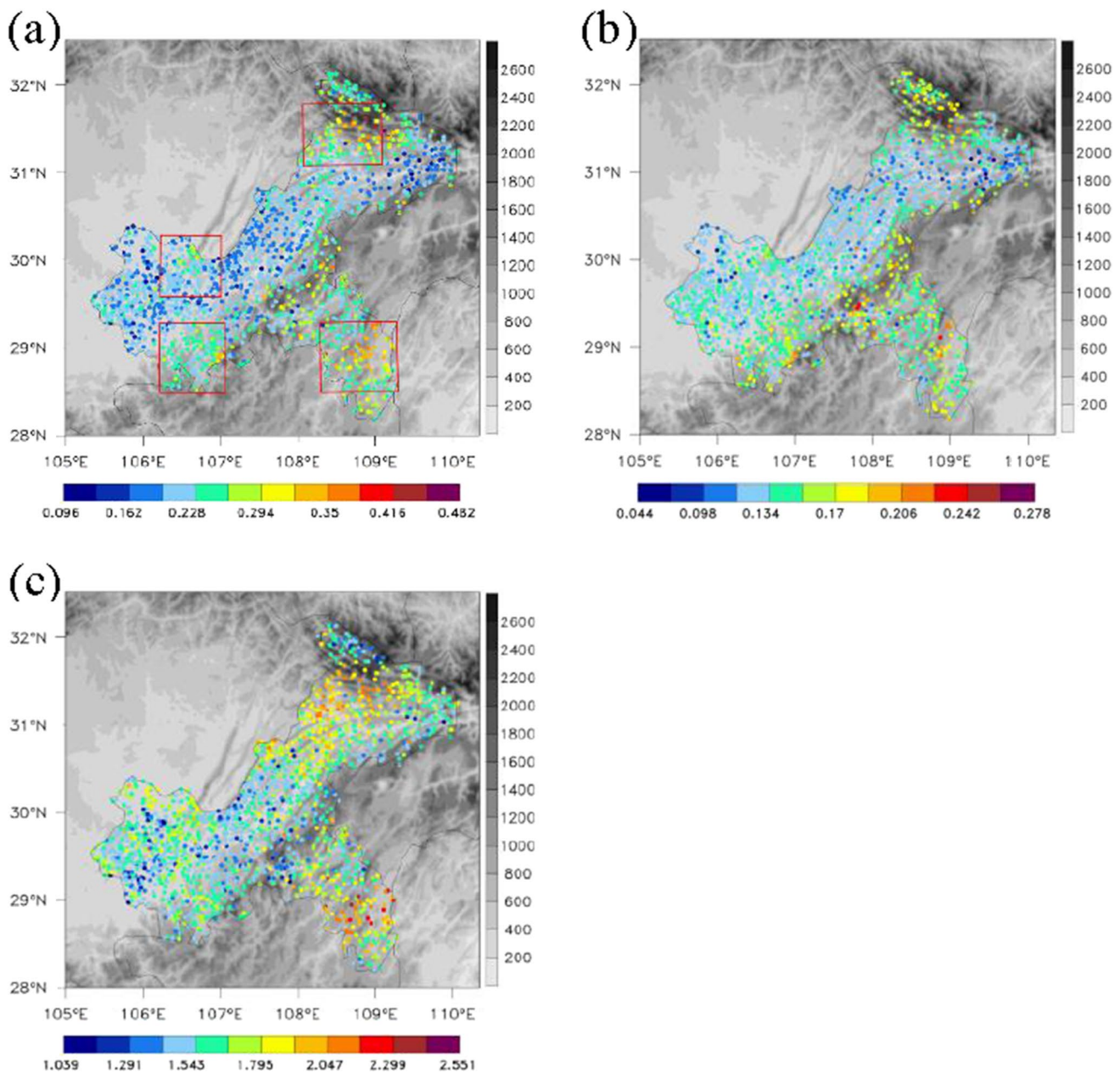


Fig. 2 Different in warm season rainfall (a) amount (colored dots; mm/h), (b) frequency (colored dots), and (c) intensity (colored dots; mm/h) during 2016–2020. Grey shadings indicate the terrain elevation

not occur at the tops of DBM and WLM but in the two slope regions. The large rainfall intensity values extend southward to the south of mountainous terrain, especially in the south DBM and the south WLM, which indicates that the terrain has a significant impact on the characteristics of precipitation. The heavy rainfall is more likely to occur in the south of the piedmont, namely the windward slope zone with the terrain interacting with the southerly wind, rather than the tops (Houze 2012). The same results are found by Chen et al. (2019) in this area. The spatial correlation coefficient between the rainfall amount and

frequency (intensity) in regions, where rainfall amount exceeds 0.23 mm/h and height ranging between 500 and 1000 m, is 0.73 and 0.65, respectively. These coefficients indicate that most stations with large rainfall amount also have high rainfall frequency.

In summary, the spatial distributions of rainfall amount, frequency, and intensity have obvious regional characteristics. It is notable that the distributions of large rainfall amount, frequency, and intensity values are located in the complex mountainous terrain areas, especially in the four study regions we have selected.

The peak time of the rainfall factors reflects the main characteristic of diurnal variation. To describe the phase of the peak time in the diurnal variation more clearly, we divided the 24 h of a day into four time periods: night (2100–0100 LST), early morning (0200–1000 LST), noon (1100–1300 LST), and afternoon (1400–2000 LST). Figure 3 shows spatial distributions of the hourly peak over 24 h for the warm season rainfall amount, frequency, and intensity. The prevailing early-morning peaks (0200–1000

LST) of rainfall amount appear over the west, the middle, the most of southeast, and the parts of northeast regions in Chongqing. The ratio of early-morning peaks accounts for up to 81.9% of all stations. The late-afternoon peaks (1400–2000 LST) mainly appear over DBM ranges and WLM ranges, and the proportion of all stations is 11.8%. In addition, the peak hours of rainfall in the western region (west of 107°E) occur obviously earlier than those in the eastern region (east of 108°E), which has been found that the

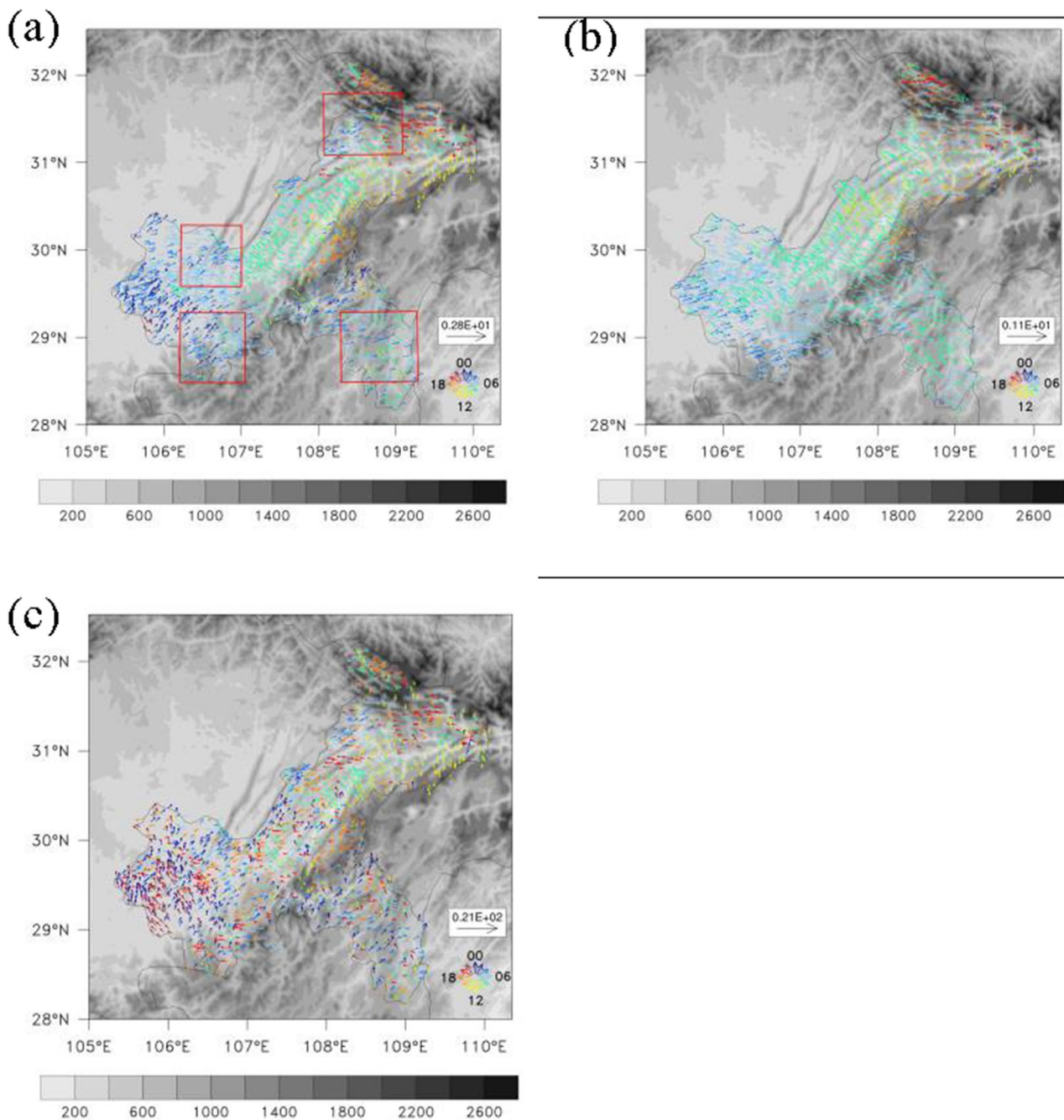


Fig. 3 Diurnal peaks of warm season rainfall (a) amount, (b) frequency, and (c) intensity during 2016–2020

eastward delay of diurnal phases downstream of the central eastern China (Yu et al. 2007b).

Similar to the rainfall amount, the early-morning peaks have played dominant role for the rainfall frequency. A total of 88.1% of the stations have early-morning peaks, which distribute over the major region. The rare late-afternoon peaks (8.6%) scatter in DBM ranges and WLM ranges. Also, it is notable that the eastward delayed diurnal phases occur mainly in the peak hours of rainfall frequency from the west to the east.

Compared with the patterns of rainfall amount and rainfall frequency, the patterns of the rainfall intensity are apparently inhomogeneous. 47.0% of the total stations have early-morning peaks, which mostly distribute over the west region and southeast region.

Overall, the above results demonstrate the dominance of early-morning peaks in determining the distinct diurnal features of warm season rainfall and the characteristics of nocturnal rainfall with eastward phase transition. In accordance with the diurnal peaks showing that the nighttime rain is evident in the SCB (Yu et al. 2007a; Bao et al. 2011; Qian et al. 2015; Zhang et al. 2019b; Li et al. 2020a, b), the same prominent nocturnal feature is found in the SW and NW, yet the diurnal peaks are not always consistent with the SE and NE. The west Chongqing with low terrain height is located in the eastern SCB, but the east Chongqing with high altitude complex terrain reaches the edge of SCB. We further analyze the detail characteristics of the four study regions in the following chapter.

3.2 The diurnal variation of precipitation in different areas

The general spatial features of the hourly warm season rainfall in Chongqing have been acknowledged. To recognize the diurnal variations in the warm season rainfall, Fig. 4 shows the standardized diurnal curves of the warm season rainfall amount, frequency, and intensity over the four study regions.

Specifically, it can be seen that the diurnal variations of rainfall amount have bimodal structure with a dominant early-morning peak at approximately 0700 LST (23 UTC) and a weaker secondary late-afternoon peak at approximately 1600 LST (08 UTC) (Fig. 4a). The proportions of early-morning rainfall amount account for 57.5%, 55.0%, 48.0%, and 44.2% of the total rainfall in the SW, NW, SE, and NE (Fig. 5a), respectively, and the percentages for late-afternoon rainfall are 19.7%, 21.4%, 23.7%, and 29.8% (Fig. 5b), respectively. Similar to the diurnal variation in the SCB showing that the nocturnal rainfall is evident (Qian et al. 2015; Zhang et al. 2019b), the difference is that the rainfall amount has bimodal peaks with the maximum peak values of the dominant early-morning

in the SW, NW, SE, and NE, and the values are 0.396, 0.404, 0.388, and 0.362, respectively, higher than that of the late afternoon, which are 0.183, 0.204, 0.251, and 0.307, respectively.

Being different from bimodal diurnal peaks of rainfall amount, there is single peak of the rainfall frequency at around 0700 LST (23 UTC) in the early-morning in the SW, NW, and SE, which accounts for 50.3%, 48.1%, and 43.4% of the total rainfall, respectively (Fig. 5b), but there are bimodal peaks that are the same as rainfall amount in the NE. The maximum peak values of the rainfall frequency in the SW, NW, SE, and NE are 0.197, 0.212, 0.191, and 0.167, respectively.

Compared with the rainfall amount and frequency, the diurnal variation of the rainfall intensity is not very evident. There is bimodal peak in the SW, which is different from the multi-peaks structure in the NW, SE, and NE with the peak values located at around 0600 LST (22 UTC) in the early morning. The detailed diurnal variation of rainfall intensity in every region is inhomogeneous.

For every region, the diurnal variations of rainfall amount can be attributed to those of both the rainfall frequency and rainfall intensity. The dominant early-morning peak mainly comes from the rainfall frequency, and the weaker secondary late-afternoon peak mainly is generated due to the rainfall intensity. Especially for the NE, such kind of rainfall is likely to occur as local convective precipitation. As noted by Liao et al. (2007), due to the diurnal variation of solar heating, the lower atmosphere tends to reach an unstable state in the afternoon so that a little disturbance can trigger local convective rainfall. Yu et al. (2013) also indicated that this occurs due to the asymmetry of precipitation processes and the evolution of convective clouds. Our findings differ from previous studies obtained from the hourly national automatic weather stations (Chen et al. 2019), which do not include more regional automatic weather stations.

In conclusion, it should be noted that the maximum peak time periods are relatively consistent with diurnal variation of rainfall amount, intensity, and frequency with generally reaching their maxima in the early morning. In addition, the detailed diurnal rainfall cycles of rainfall amount and intensity are the same in the SW and NW, and that is generally consistent with the SE and NE.

From the above analysis, the dominant early-morning peak is evident. Some researchers found an increasing amount of precipitation with altitude increasing in the mountain (Giorgi et al. 1997; Liu et al. 2011; Guo et al. 2016). To quantitatively assess the relationship between the early-morning rainfall and the gauge elevation over the four study regions, we study the correlation between the proportion of rainfall amount (frequency) in the early morning to the total daily rainfall amount (frequency) and the gauge

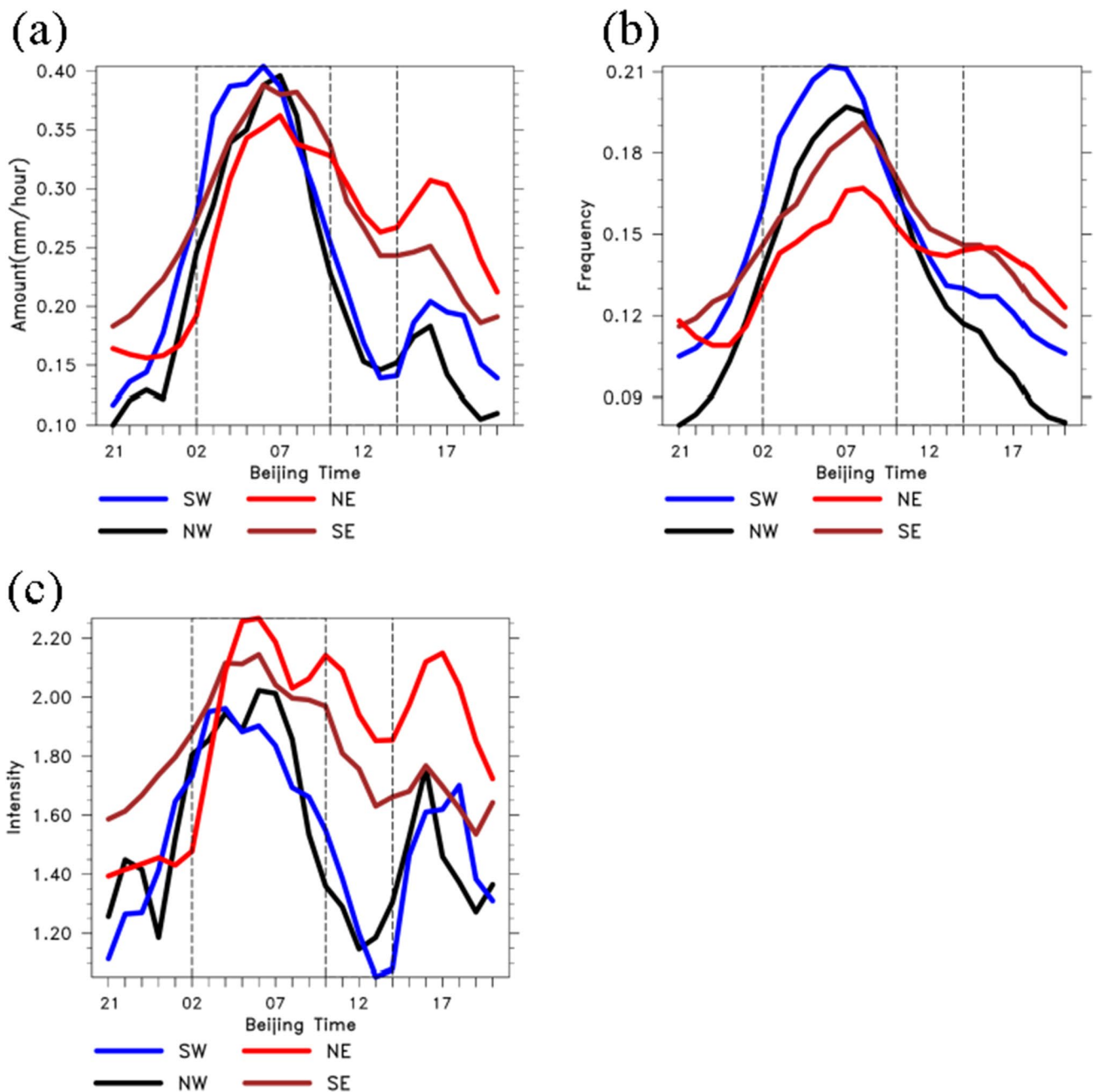


Fig. 4 Diurnal variations in warm season for the four regions rainfall (a) amount, (b) frequency and (c) intensity. The black dashed lines denote night (2100–0100 LST), early-morning (0200–1000 LST), noon (1100–1300 LST), and afternoon (1400–2000LST) period

elevation (Fig. 6). The linear fittings show that the proportion of the rainfall amount (frequency) occurring during the early-morning period is negatively correlated with the elevation in four regions. The linear correlation coefficients (R) are -0.934 (-0.934), -0.880 (0.886), -0.902 (-0.906), and -0.814 (-0.814), respectively, which pass the significance test at the 99% confidence level, and correspond to the proportions of early-morning rainfall amount

(frequency) to the total rainfall at the higher elevations to be smaller than that at the lower elevations. This suggests that the altitude effect of the early-morning rainfall frequency is significant. The main characteristics of diurnal variation of early-morning rainfall obviously diminish as elevation increases, and this phenomenon indicates that more rainfall in the higher mountainous regions occurs in other periods.

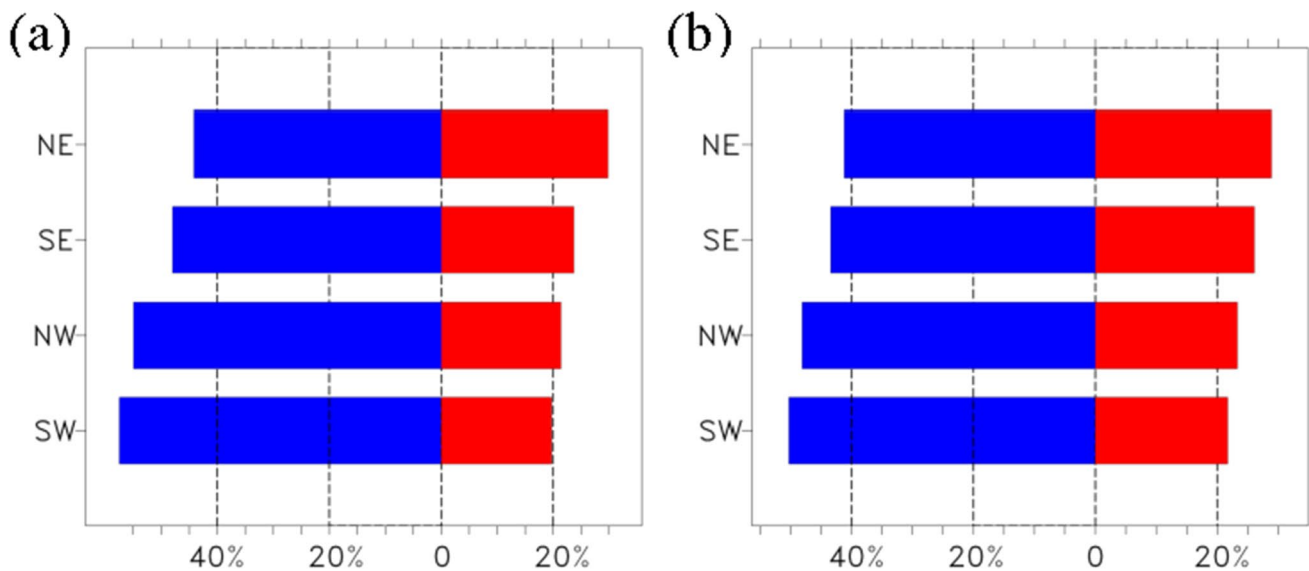


Fig. 5 The proportions of rainfall (a) amount and (b) frequency in the early-morning (blue bars; %) and late-afternoon (red bars; %) period to their daily rainfall for the four regions

3.3 The detailed characteristics of early-morning rainfall in four regions

The previous results demonstrate the dominance of early-morning rainfall in determining the distinct diurnal features of warm season rainfall. To reveal detailed spatial distribution of rainfall features in the four study regions during early morning, the regions with the most obvious signals were selected, and every region is divided to 4 sub-regions with considering the combination of mountains extending direction and the terrain height variation from the lower to the higher elevation. The mountains stretch from southwest to northeast in the NW, simultaneously, the heights gradually increase. The altitude of mountains gradually increases from west to east in the SW. The mountains present south-north-oriented extending with the terrain height gradually increasing in the SE. The altitude of mountains increases from south to north in the NE.

The spatial patterns of rainfall amount (Fig. 7) during early morning are considerably similar to that of the warm season rainfall amount (Fig. 2). It is notable that the rainfall amount approximately increases as the terrain height increases in the four study regions. In every study region, the relatively small value stations of rainfall amount are located in the first sub-region, and the large value stations mainly concentrate in the fourth sub-region. In the NW and the SE, the rainfall amount gradually increases along the direction of mountains, especially in the south side of mountains. In the SW and the NE, the rainfall amount gradually increases from the foot to the top of mountains.

For more detailed investigation of the rainfall variations in the four study regions, Fig. 8 presents variations of the rainfall amount for four sub-regions in every study region at the different elevation. Along the mountains from southwest to northeast, the average elevations of the sub-regions stations increase from 346.1 to 536.4 m in the NW (Fig. 8a), but there is a slight decrease in sub-region 2. Meanwhile, the mean, median, upper quartile, and maximum values of rainfall amount in 4 sub-regions also increase, ranging from 0.315, 0.313, 329, and 0.363 mm/h, in the first sub-region, to 0.378, 0.380, 0.397, and 0.470 mm/h, respectively, in the fourth sub-region. In the SW (Fig. 8b), the average terrain heights gradually increase from 405.5 to 666.5 m, and the mean (0.344 mm/h) and median (0.345 mm/h) values in westernmost sub-region increase to 0.383 and 0.376 mm/h in the easternmost sub-region. In addition, we should notice that the mean and median values in the second sub-region are slightly smaller than those in the first sub-region, which are influenced by the stations in the low altitude terrain, but the slightly different variation does not affect the overall change with terrain height. The mean, median, and minimum values of rainfall amount in the southernmost region are 0.316, 0.319, and 0.266 mm/h, respectively, whereas those in the northernmost region reach 0.427, 0.436, and 0.378 mm/h, respectively, in the SE. For the rainfall amount, practically all statistics increase along the mountain extending in the SE (Fig. 8c). Simultaneously, the average elevations of the sub-regions stations gradually increase from 431.7 to 719.9 m. Figure 6d also presents the obvious feature that is the rainfall amount consistent variations

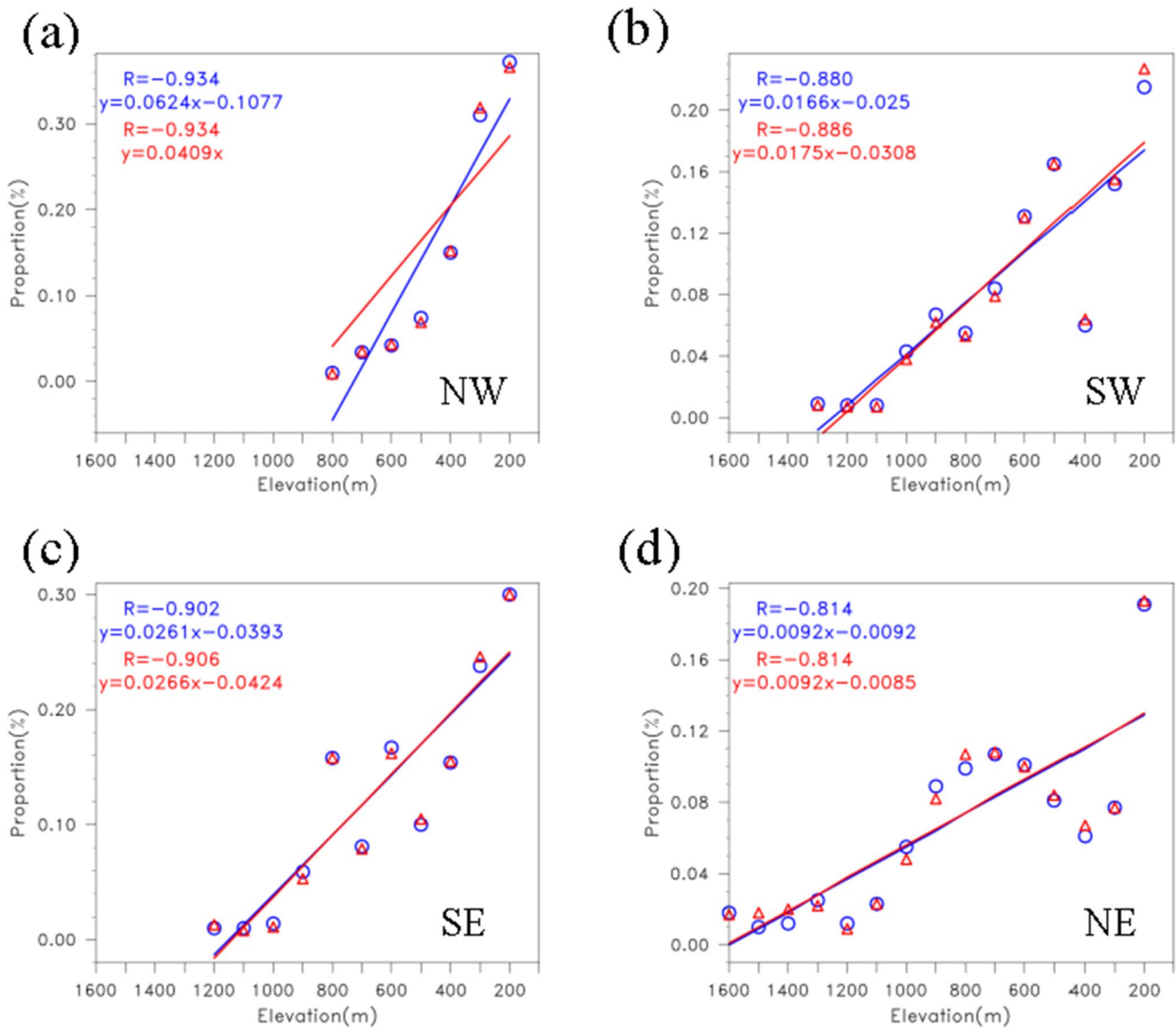


Fig. 6 Relationships between the elevation and the proportion of early-morning rainfall frequency (blue) and amount (red) in (a) NW, (b) SW, (c) SE, (d) NE regions, the points represent the proportion

values of early-morning rainfall amount (frequency) to their daily rainfall within each 100 m. The colored lines mean the linear fitting

with elevation increasing. The mean rainfall amount in the southernmost region is only 0.247 mm/h, whereas that in the northernmost region reaches 0.398 mm/h.

Boxplot of stations rainfall amount in the four study regions mostly shows the characteristics of consistent variations as the terrain heights increase. The results show that terrain elevation plays an important role in affecting the regional distribution of rainfall amount. The NW denotes the complex topography of mixed basin and hills, and the SW represents the mountainous terrain in southwest Chongqing adjacent to the northern DLM. The underlying surface is mainly hilly, and the average elevations of the sub-regions stations are relatively low in the sub-regions 1 and 2 of the

NW and the SW, so the rainfall amount of these stations are relatively lower. The underlying surface is mainly mountainous terrain, and the average elevations of the sub-regions stations are relatively high in the sub-regions 3 and 4, therefore, resulted in the rainfall amount values are relatively high. The underlying surface is mainly mountainous terrain, and the average elevations of the sub-regions stations increase sharply from the sub-region 2 to 3 in the SE, so the rainfall amount increases sharply. Compared with the others three study areas, the average elevations gradually increase from the sub-region 1 to 4 in the SE, and the increase gradient is relatively consistent, so the rainfall amount gradually increases.

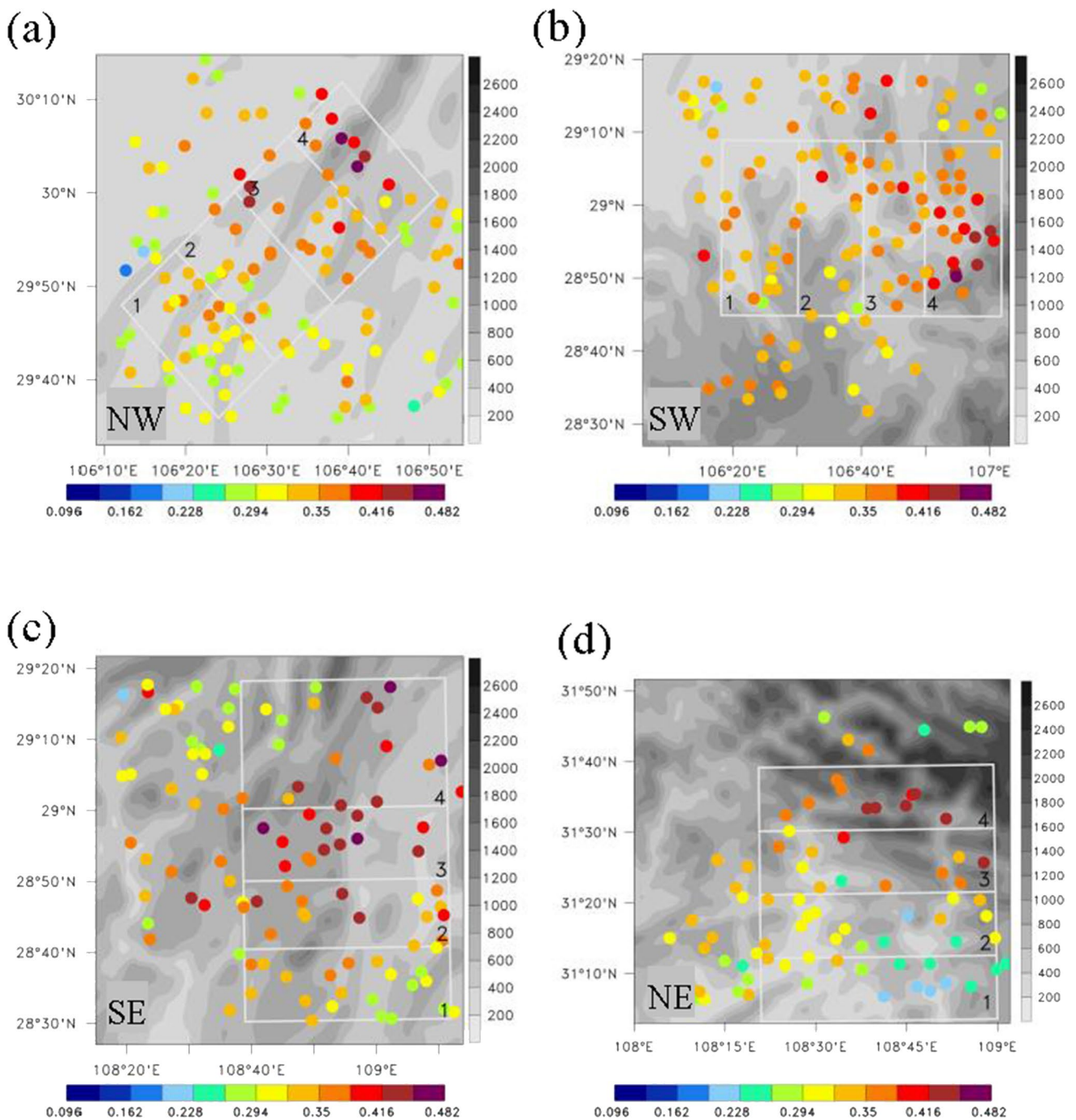


Fig. 7 The spatial distribution of rainfall amount (units: mm/h) in warm season during early-morning (0200–1000 LST) in (a) NW, (b) SW, (c) SE, (d) NE regions. Grey solid lines (black numbers) outline the borders (label the number) of every sub-region

Similar to rainfall amount, the rainfall frequency also shows different spatial variations in the four study regions (Fig. 9). The rainfall frequency also gradually increases as the terrain height increases. The small value stations of rainfall amount are located in the first sub-region, and the large stations are concentrated in the fourth sub-region. The rainfall frequency has a clearer

increase along the extending direction of mountains in the NW and the SE, and those also have a similar increasing trend with the terrain height gradually increasing from the low inlands to the high hills of mountains in the SW and the NE. The values at the top of mountains are also bigger than those at the foot at same longitudes or latitudes.

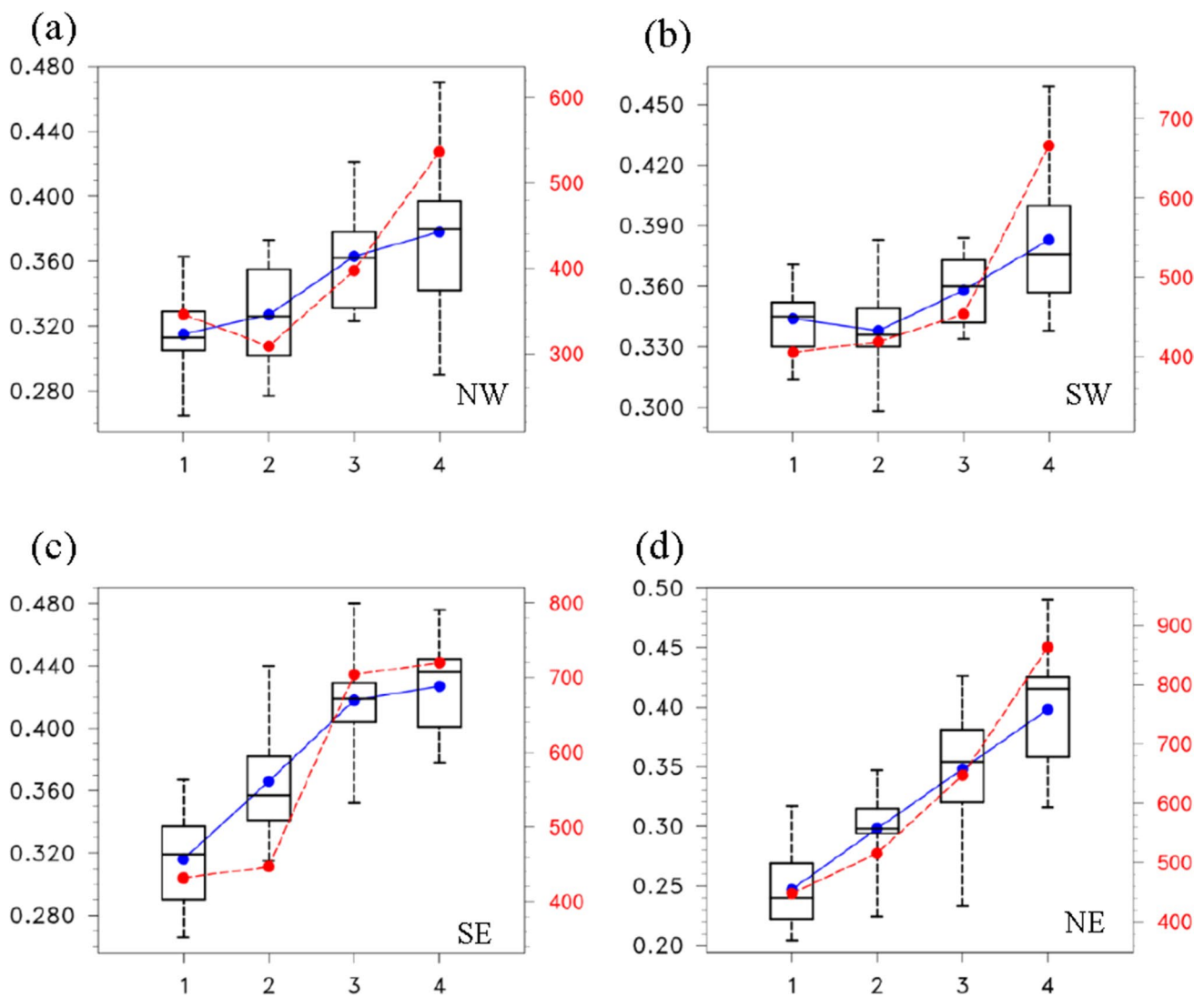


Fig. 8 Boxplot of rainfall amount (units: mm/h) during early morning of (a) NW, (b) SW, (c) SE, (d) NE regions; box shows lower and upper quartiles. Black lines inside boxes represent medians. Blue dots are for data averages. Minimum and maximum values are shown by

whiskers. Red line represents mean elevation (units: m) of all stations. Labels 1, 2, 3, and 4 at bottom x-axis represent four sub-regions in the four study regions. The left y-axis label means rainfall amount scales and the right y-axis label indicates the elevation scales

The detailed rainfall frequency changes correspondingly with the topographic elevation, as shown in Fig. 10. In the southwest-northeast direction in the NW (Fig. 10a), the rainfall exhibits consistent variations with elevation, in terms of rainfall amount and frequency. The mean rainfall frequency is 0.174 in the first sub-region; however, it reaches 0.191 in the fourth sub-region. In the SW (Fig. 10b), from west to east along the mountains, the mean terrain heights are 405.5, 418.9, and 453.9 m, respectively, increasing at interval of approximately 50 m, but the elevations increase to 666.5 m in 4 sub-region, more than 200 m higher than those in 1–3 sub-regions. Due to the terrain heights variation, the mean and median stay relatively consistent in 1–3 sub-regions (0.187, 0.188), but

that obviously increases in the fourth sub-region (0.207, 0.203). The mean (0.169) and median (0.173) values in southernmost sub-region increase 0.210 and 0.210 compared with those in northernmost sub-region in the SE (Fig. 10c). Meanwhile, it should be noted that the mean and median values are slightly smaller in the second sub-region than those in the first sub-region, but the slight difference does not affect the overall variation tendency. There is an increase in the rainfall frequency concurrent with the increasing elevations over 1–4 sub-regions in the NE. The mean, median, upper quartile, and maximum values increase, ranging from 0.134, 0.135, 0.139, and 0.151, respectively, in the first sub-region to 0.183, 0.178, 0.193, and 0.260, respectively, in the fourth sub-region.

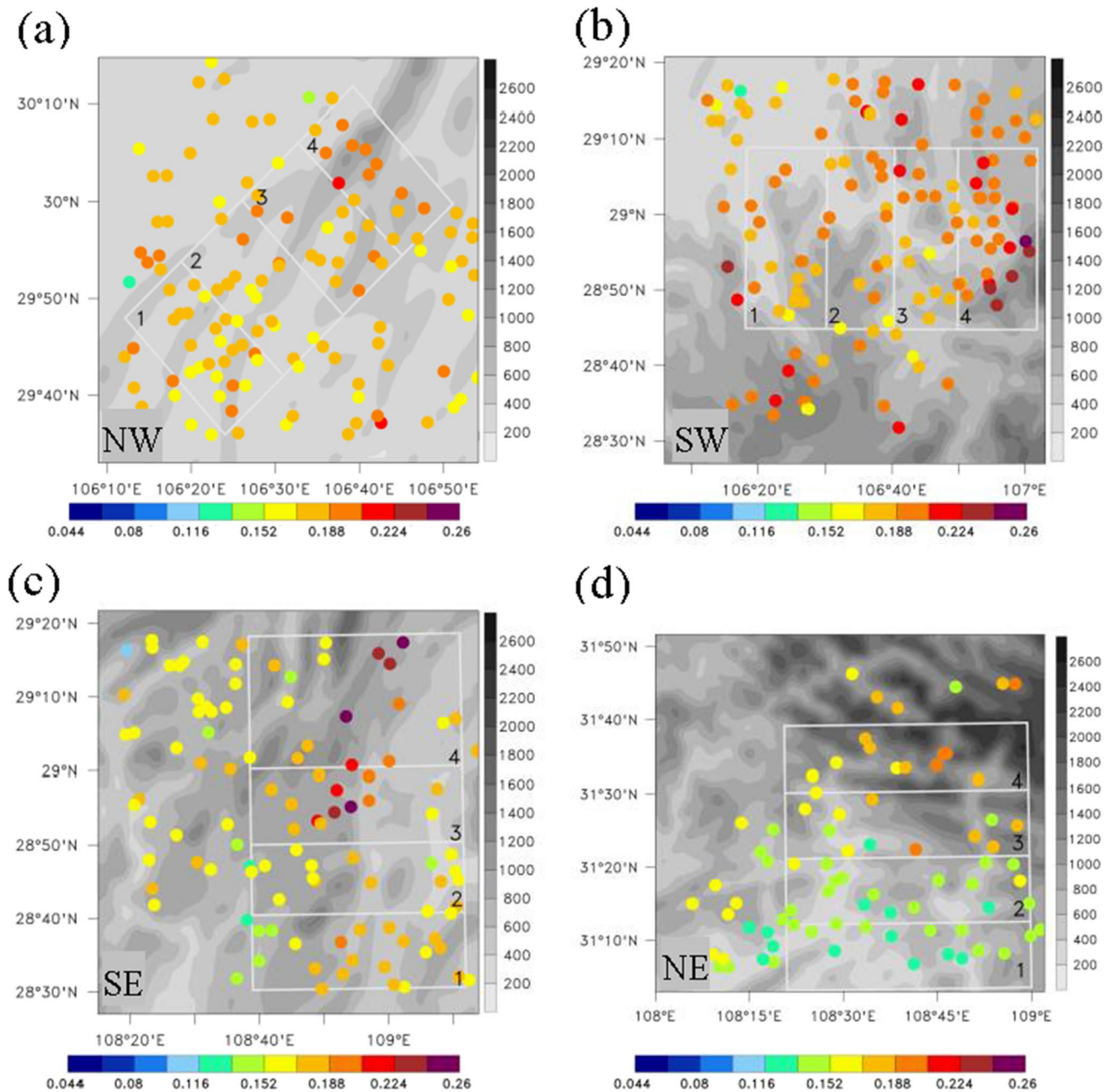


Fig. 9 The same as Fig. 7, but for rainfall frequency

Boxplots of rainfall frequency of stations in the four study regions mostly show the consistent variations with rainfall amount. The rainfall frequency values of stations are relatively low in the sub-region 1 and 2 of NW and SW, but high in the sub-region 3 and 4. The rainfall frequency values increase sharply from the sub-region 2 to 3 in the SE. The rainfall frequency values gradually increase from the sub-region 1 to 4 in the SE.

From the above discussion of the spatial variations of the rainfall over four focus regions, the results show that the rainfall amount and frequency at higher elevations are larger than those

at lower elevations, and the rainfall amount and frequency significantly increases as the terrain height sharply increase, which indicates that mountainous terrain has a remarkable enhancing effect on precipitation in the four study regions.

3.4 The diurnal variation of rainfall events in different areas

To explore the relationships between rainfall occurring time and the duration hours of the rainfall events, the rainfall

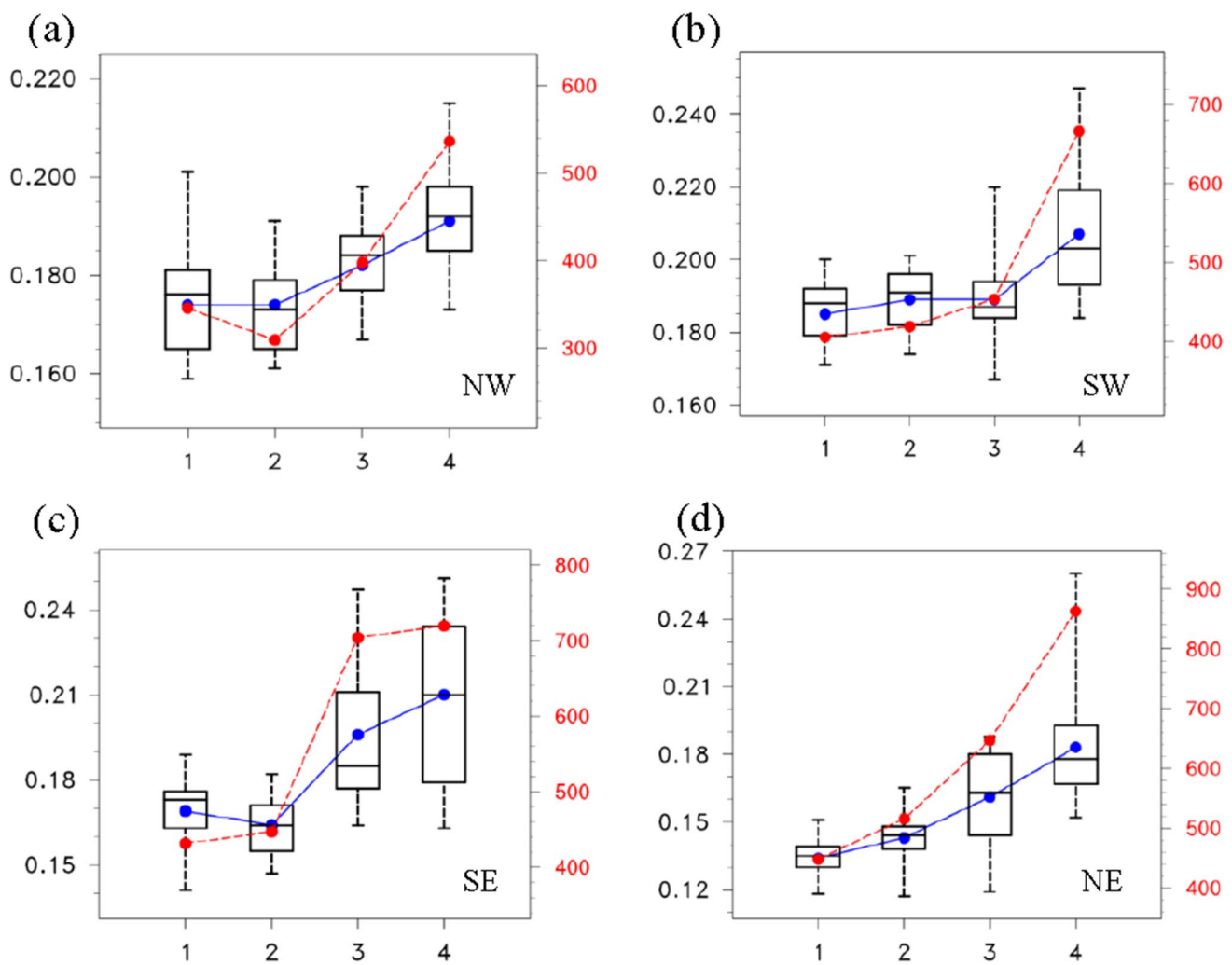


Fig. 10 The same as Fig. 8, but for rainfall frequency

amount and frequency decomposed by duration and diurnal phase for the four study regions are analyzed, which are normalized by the daily mean of each duration time. In the NW (Fig. 11a), rainfall events with duration hours of less than 6 h reach their peaks at roughly 0400 LST in the early morning. Rainfall events lasting more than 6 h tend to peak between 0200 and 0400 LST. However, it can be seen clearly that the amount and frequency of rainfall events that last longer than 6 h is higher than that of lasting less than 6 h, and this kind of rainfall occurs mostly in the early morning. In the SW (Fig. 11b), rainfall event with duration less than 6 h reaches its peak at roughly 2000 LST in the afternoon, and a less pronounced second peak is observed at 0400 LST in the early morning. Rainfall events lasting more than 6 h tend to peak between 0200 and 0400 LST. Similar results are found in the SE (Fig. 11c), though rainfall with lasting less than 6 h reaches its peak at roughly 0000 LST in the

midnight. In the NE (Fig. 11d), rainfall events lasting less and more than 6 h mainly occur in the nighttime.

From the above analysis, short-duration rainfall events (1–6 h) tend to start between afternoon and night, while long-duration rainfall events (> 6 h) tend to start in the night. Nocturnal rainfall events tend to begin simultaneously while long-duration rainfall ends later, showing that long-duration rainfall events make a larger contribution to total rainfall amount. The duration is closely related to the physical mechanisms of precipitation.

Yu et al. (2007a) revealed that the diurnal cycle of long-duration precipitation exhibits an early-morning maximum while short-duration precipitation an afternoon to evening maximum. The late-afternoon maximum can be explained by surface solar heating, which results in maximum low-level atmospheric instability and thus moist convection in the afternoon (Chen et al. 2019). The nocturnal maximum

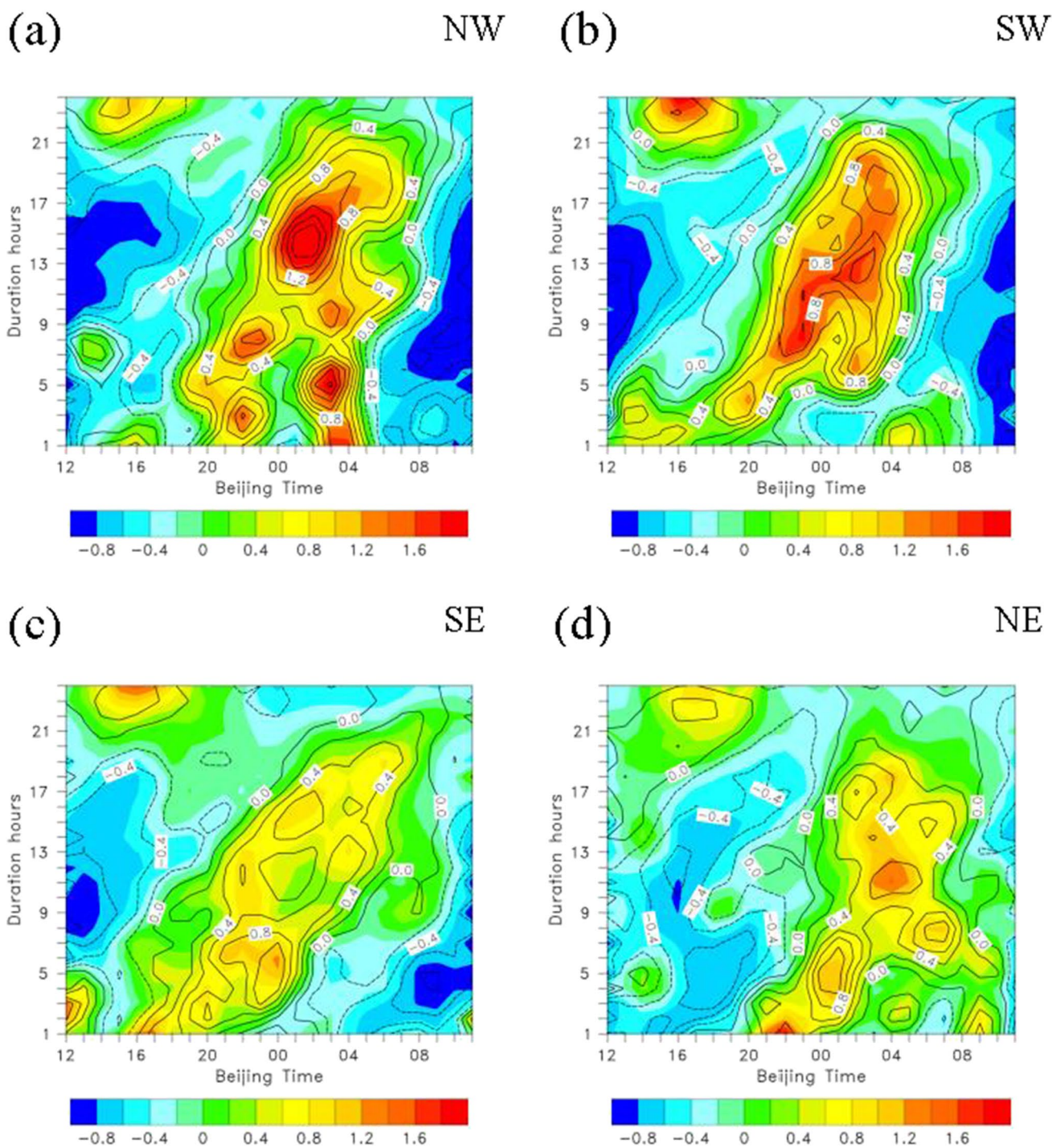


Fig. 11 Diurnal cycle of rainfall events of rainfall amount (shaded) and frequency (contours) with change of different duration in (a) NW, (a) SW, (a) SE, and (c) NE. The rainfall amount and frequency is normalized by the daily mean for each duration time

may result from the diurnal variation of local circulation forced by the complex terrain.

Similar to Fig. 5, the proportions of two main periods for rainfall events with different durations are shown for the four regions (Fig. 12). When the duration is between 1 and

3 h, the rainfall frequency proportion (25.6%) in the early-morning period is greater than that (17.1%) in the late-afternoon period in the NW (Fig. 12a), but the rainfall amount proportion (4.5%) in the early morning is slightly smaller than that (5.8%) in the late afternoon. The rainfall frequency

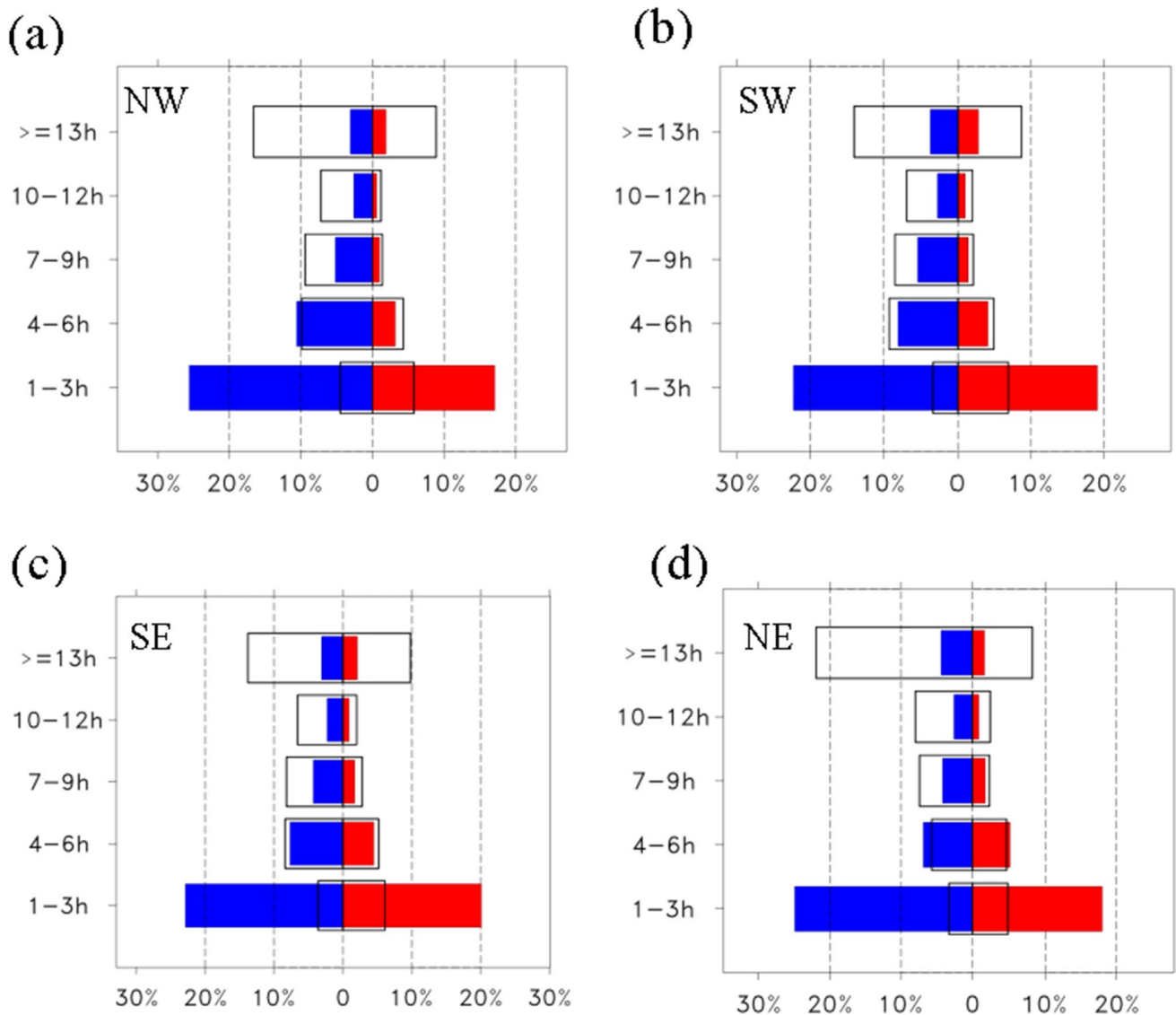


Fig. 12 The proportions of rainfall amount (black rectangle; %) and frequency (bar; %) events during different durations to their daily rainfall events in the (a) NW, (a) SW, (a) SE, and (c) NE. The blue

bars represent the proportion values of the early-morning period, and the red bars indicate the late-afternoon period

proportion of durations of 4–6 h (10.6%), 7–9 h (5.2%), 10–12 h (2.6%), and more than or equal to 13 h (3.1%) in the early-morning period are roughly triple as much as that in the late-afternoon period, which are 3.2%, 1.0%, 0.6%, and 1.9%, respectively. The rainfall amount proportion of durations of 4–6 h (9.9%), 7–9 h (9.4%), 10–12 h (7.2%), and more than or equal to 13 h (16.6%) in the early-morning period are roughly twice as much as that in the late-afternoon period, which are 4.3%, 1.4%, 1.2%, and 8.9%, respectively.

Similar results are shown in the following three regions. For proportions of rainfall events, more than 35% short-duration rainfall (1–6 h) events happen during the early-morning period. When the duration is above 7 h, the frequency

proportion is slightly greater than 10%, accounting for 33.2% of the total rainfall.

Although the diurnal large value zones of rainfall events in the four regions appear in the early morning, the detailed diurnal rainfall cycles are different. We will further analyze the peak time characteristics of rainfall events with different duration in the following passages.

The peak of long persistent precipitation is usually in the morning, which accounts for more than 60% of precipitation in central and eastern China, while short persistent precipitation mainly appears in the afternoon (Yu et al. 2007a). The occurrence of the rainfall maximum is important for rainfall events (Yu et al. 2013). To quantitatively assess the relationship between the gauge elevation and the

early-morning maximum rainfall, Fig. 13 shows the relationships of the gauge elevation and the proportion of rainfall maximum frequency during the early-morning period to the total daily rainfall frequency trend magnitude. There are obviously negative correlations between the magnitude of proportion trends and the elevation in four regions. The linear correlation coefficients (R) are -0.932 , -0.878 , -0.914 , and -0.803 above the 99% confidence level, respectively. It means that the proportions of early-morning rainfall maximum frequency to the total rainfall at the higher elevations are smaller than that of the lower elevations. This suggests that the altitude effect on the early-morning rainfall maximum frequency is significant. The early-morning rainfall maximum trend significantly diminishes with elevation,

which indicates that higher mountainous areas experience more other raining periods than that at lower elevations.

4 Conclusions and discussion

Based on the hourly rain gauge data of high-density stations in Chongqing during the warm season (May to September) from 2016 to 2020, the overall features and regional differences in the diurnal variations of rainfall affected by complex terrain are identified, and the detailed influences of the gauge elevations on the diurnal variations of rainfall are also investigated. The main conclusions can be summarized as follows.

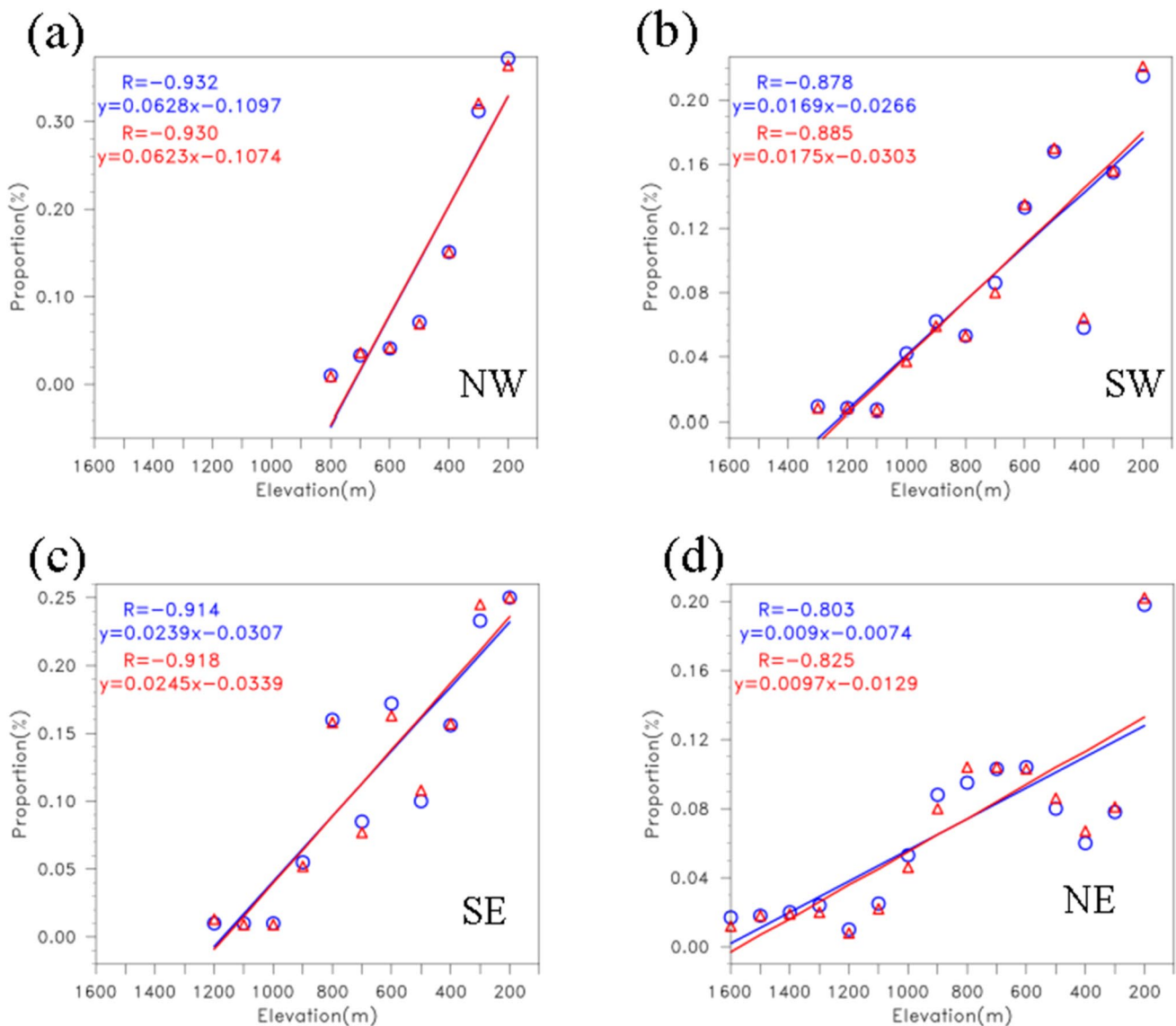


Fig. 13 The same as Fig. 6, but for the proportion of early-morning rainfall maximum frequency (blue) and amount (red) to their daily rainfall events in (a) NW, (b) SW, (c) SE, (d) NE regions

- (1) The spatial features of rainfall amount, frequency, and intensity have obvious regional characteristics under the influence of complex terrain in Chongqing. The stations with larger rainfall amount, frequency, and intensity values are located in the higher complex mountainous terrain areas. The detailed characteristics of the four study regions show that the rainfall amount and frequency at higher elevations are larger than those at lower elevations, and they significantly increase, especially in the direction that terrain height sharply increases along mountains extending.
- (2) The diurnal characteristics of rainfall amount, frequency, and intensity have obvious regional characteristics. The maximum peak time periods are relatively consistent in reaching their maxima in the early-morning. The early-morning peaks play a dominant role for the rainfall frequency and amount, which account for 81.9% and 88.1% of all stations, respectively. The patterns of the rainfall intensity are apparently inhomogeneous. The rainfall amount has bimodal structure with a dominant early-morning peak at approximately 0700 LST (23 UTC) and a weaker secondary late-afternoon peak at approximately 1600 LST (08 UTC). There is a single peak diurnal characteristic of the rainfall frequency in the SW, NW, and SE, while bimodal peak in the NE.
- (3) The gauge elevation has a significant impact on the diurnal variations of the early-morning rainfall. As elevation decreases, the proportion of rainfall amount (frequency) that occurs during early-morning periods increase in the four study regions. In other words, the early-morning peak dominates in low elevations areas, while the high mountainous areas experience more other raining periods than that at lower elevations. The same pattern is found in the proportions of early-morning rainfall maximum frequency to the total rainfall events.
- (4) Different duration hours of rainfall events have distinct diurnal variation and phase features. Short-duration rainfall tends to start between afternoon and night, while long-duration rainfall tends to start in the night. Nocturnal rainfall events tend to begin simultaneously, while long-duration rainfall ends later. Consequently, long-duration rainfall events make a greater contribution to total rainfall amount.

In this study, our results indicate that the diurnal variation of rainfall in Chongqing is significantly affected by topography and demonstrates the dominance of early-morning rainfall in determining the distinct diurnal features of warm season rainfall. Prevailing nocturnal precipitation over the eastern Tibetan Plateau and its eastern periphery was discussed previously (Bai et al. 2008; Chen et al. 2009; Huang

et al. 2010; Guo et al. 2016), but the underlying mechanisms remain unclear. Jin et al. (2013) suggested that the early night precipitation peak over the western SCB was largely caused by strong ascending motion over the TP and its eastern lee side, while multiple coexisting factors contributed to the late night peak of precipitation over the central and eastern SCB. The mountain–plain solenoid circulation, driven by the inhomogeneous diabatic heating associated with topographic forcing, contributes to the nocturnal precipitation over the SCB (Zhang et al. 2014b; Qian et al. 2015). In the early evening, anomalous easterly flow moves toward the TP and causes low-level convergence over the western SCB, resulting in nocturnal precipitation over the SCB (Sun and Zhang 2012; Chen et al. 2017; Zhang et al. 2019a). Prominent diurnal inertial oscillations of south-southwesterly low-level jet into the southeast side of the SCB play an important role in modulating the diurnal variation of precipitation over the SCB (Zhang et al. 2019b). Qian et al. (2015) found that the precipitation over the SCB propagates northeastward in the early night and decays. As mentioned before, the west Chongqing goes into the SCB, in which the diurnal variation of rainfall is the same as in the SCB, while the eastern and middle Chongqing are located in the mountainous area surrounding the basin and gradually rise eastward with high terrain spreading on the WM. Chen et al. (2019) investigated the interval of precipitation associated with the diurnal distribution of lightning and revealed that the enhancement of precipitation in the mountainous area was mainly caused by the short-time strong rainfall resulting from the convection. However, these studies are limited by the use of only station observations, due to the limited data length, the inhomogeneous spatial distribution of the stations, and scarce records of rainfall in mountainous area, which cannot fully reveal the interactions between the local topography and mesoscale processes in the generation of heavy rainfall.

It is noteworthy that there are obvious regional characteristics in the diurnal variations of rainfall. The study could be helpful in further understanding the precipitation characteristics in Chongqing and in researches on precipitation over complex terrain in the southwest China. The diurnal rainfall cycles of rainfall amount and intensity are the same in the SW and NW, and they are generally consistent with those in the SE and NE. The SW and NW are located in the west Chongqing and go deep into the SCB at low elevation. The east Chongqing gradually rises with high terrain, in which the SE and NE are located. The elevation is an obvious different topographical factor. The rainfall amount and frequency significantly increase as the terrain height sharply increases, especially in the NE. The direction of orographic slope is north–south orientation where the windward slope zone interacts with the south wind. The detailed rainfall characteristics are also different in the sub-regions over the four study regions. These differences in the sub-regions

imply that apart from the elevation, some other topography-related factors, such as orographic slope and orientation, should also be considered when investigating the influence of topography on the diurnal variations of rainfall. Due to the few stations sparsely distributed mountainous areas, it is difficult to obtain detailed circulation characteristics and truly understand physical processes behind these differences in complex terrain area. Therefore, further studies are needed to validate the results by using other high-resolution data, including the high-resolution satellite data, and high-resolution numerical experiments that should be designed and carried out in future works.

Author contribution Li Qiang analyzed the data, made the figures, and wrote the paper. Zheng Yongguang and Zhou Guobing gave scientific advice and helped improve the paper. Zhu Yan and Liu Chao revised the language and characters. All the authors contributed to the discussion and final version of the paper. All authors read and approved the final manuscript.

Funding This research was supported by the National Key R&D Program of China (Grants 2018YFC1507504 and 2017YFC1502003), Chongqing Natural Science Foundation of China (cstc2021jcyj-msxmX0057), Chongqing Technology Innovation and Application Project (cstc2018jscx-msybX0162 and cstc2019jscx-msxmX0297), the Business Technology Research Project of Chongqing Meteorological Bureau (YWJSGG-202120), State Grid Chongqing Electric Power Company Science and Technology Project (2020 Yu Electric Branch 31) and Innovation and Development Project of China Meteorological Administration (CXFZ2022J011).

Data availability All data used during the study appear in the submitted supporting data.

Code availability Code generated or used during the study are available from the corresponding author on reasonable request.

Declarations

Ethics approval Not applicable.

Consent to participate Not applicable.

Consent for publication Not applicable.

Competing interest The authors declare no competing interests.

Open Access This article is licensed under a Creative Commons Attribution 4.0 International License, which permits use, sharing, adaptation, distribution and reproduction in any medium or format, as long as you give appropriate credit to the original author(s) and the source, provide a link to the Creative Commons licence, and indicate if changes were made. The images or other third party material in this article are included in the article's Creative Commons licence, unless indicated otherwise in a credit line to the material. If material is not included in the article's Creative Commons licence and your intended use is not permitted by statutory regulation or exceeds the permitted use, you will need to obtain permission directly from the copyright holder. To view a copy of this licence, visit <http://creativecommons.org/licenses/by/4.0/>.

References

- Bai AJ, Liu CH, Liu XD (2008) Diurnal variation of summer rainfall over the Tibetan Plateau and its neighboring regions revealed by TRMM multi-satellite precipitation analysis. *Chinese J Geophys* 51:518–529. <https://doi.org/10.1002/cjg2.1242>
- Bao XH, Zhang FQ, Sun JH (2011) Diurnal variations of warm-season precipitation east of the Tibetan Plateau over China. *Mon Wea Rev* 139:2790–2810. <https://doi.org/10.1175/mwr-d-11-00006.1>
- Barros AP, Lang TJ (2003) Monitoring the monsoon in the Himalayas: Observations in central Nepal, June 2001. *Mon Wea Rev* 131:1408–1427. [https://doi.org/10.1175/1520-0493\(2003\)131%3c1408:MTMITH%3e2.0.CO;2](https://doi.org/10.1175/1520-0493(2003)131%3c1408:MTMITH%3e2.0.CO;2)
- Basist A, Bell GD, Meentemeyer V (1994) Statistical relationships between topography and precipitation patterns. *J Clim* 7:1305–1315. [https://doi.org/10.1175/1520-0442\(1994\)007%3c1305:SRBTAP%3e2.0.CO;2](https://doi.org/10.1175/1520-0442(1994)007%3c1305:SRBTAP%3e2.0.CO;2)
- Burbank DW, Blythe AE, Putkonen J, Pratt-Sitaula B, Gabet E, Oskin M, Barros A, Ojha TP (2003) Decoupling of erosion and precipitation in the Himalayas. *Nature* 426:652–655. <https://doi.org/10.1038/nature02187>
- Chen CS, Lin YL, Zeng HT, Chen CY, Liu CL (2013) Orographic effects on heavy rainfall events over northeastern Taiwan during the northeasterly monsoon season. *Atmos Res* 122:310–335. <https://doi.org/10.1016/j.atmosres.2012.10.008>
- Chen H, Li J, Yu RC (2018) Warm season nocturnal rainfall over the eastern periphery of the Tibetan Plateau and its relationship with rainfall events in adjacent regions. *Int J Clim* 38:4786–4801. <https://doi.org/10.1002/joc.5696>
- Chen GX, Sha WM, Iwasaki T, Wen ZP (2017) Diurnal cycle of a heavy rainfall corridor over East Asia. *Mon Wea Rev* 145:3365–3386. <https://doi.org/10.1175/MWRD-16-0423.1>
- Chen GX, Sha WM, Iwasaki T (2009) Diurnal variation of precipitation over southeastern China: spatial distribution and its seasonality. *J Geo Res* 114:D13103. <https://doi.org/10.1029/2008jd011103>
- Chen SY, Yan Y, Liu G, Fang DX, Wu Z, He J, Tang JP (2019) Spatiotemporal characteristics of precipitation diurnal variations in Chongqing with complex terrain. *The App Clim* 137:1217–1231. <https://doi.org/10.1007/s00704-018-2662-7>
- Chen WJ, Chen CH, Li LB, Xing LT, Huang GR, Wu CH (2015) Spatiotemporal analysis of extreme hourly precipitation patterns in Hainan Island, South China. *Water* 7:2239–2253. <https://doi.org/10.3390/w7052239>
- Chen Y, Wang X, Huang L, Luo Y (2021) Spatial and temporal characteristics of abrupt heavy rainfall events over Southwest China during 1981–2017. *Int J Clim* 41:3286–3299. <https://doi.org/10.1002/joc.7019>
- China Meteorological Administration (2003) Specifications for surface meteorological observation. China Meteorol. Press, Beijing
- Chongqing Bureau of Geology and Minerals Exploration (CBGM) (2002) Structure outline map of Chongqing and instruction. Geological Publishing House (in Chinese)
- Colle BA (2004) Sensitivity of orographic precipitation to changing ambient conditions and terrain geometries: An idealized modeling perspective. *J Atmos Sci* 61:588–606. [https://doi.org/10.1175/1520-0469\(2004\)061%3c0588:SOOPTC%3e2.0.CO;2](https://doi.org/10.1175/1520-0469(2004)061%3c0588:SOOPTC%3e2.0.CO;2)
- Couto FT, Ducrocq V, Salgado R, Costa MJ (2016) Numerical simulations of significant orographic precipitation in Madeira island. *Atmos Res* 169:102–112. <https://doi.org/10.1016/j.atmosres.2015.10.002>
- Cuo L, Zhang YX (2017) Spatial patterns of wet season precipitation vertical gradients on the Tibetan Plateau and the surroundings. *Sci Rep* 7:5057. <https://doi.org/10.1038/s41598-017-05345-6>

- Dai A, Giorgi F, Trenberth KE (1999) Observed and model simulated diurnal cycles of precipitation over the contiguous United States. *J Geophys Res* 104:6377–6402. <https://doi.org/10.1029/98jd02720>
- DeHart JC, Houze RA (2017) Orographic modification of precipitation processes in Hurricane Karl (2010). *Mon Wea Rev* 145:4171–4186. <https://doi.org/10.1175/MWR-D-17-0014.1>
- Deshpande NR, Kulkarni A, Krishna Kumar K (2012) Characteristic features of hourly rainfall in India. *Int J Clim* 32:1730–1744. <https://doi.org/10.1002/joc.2375>
- Fu PL, Zhu KF, Zhao K, Zhou BW, Xue M (2019) Role of the nocturnal low-level jet in the formation of the morning precipitation peak over the Dabie mountains. *Adv Atmos Sci* 36:15–28. <https://doi.org/10.1007/s00376-018-8095-5>
- Gan YT, Li NN, Li J (2019) Differences in the rainfall characteristics between Mount Tai and its surrounding areas. *J Meteor Res* 33:976–988. <https://doi.org/10.1007/s13351-019-9006-0>
- Giorgi F, Hurrell JW, Marinucci MR, Marinucci MR (1997) Elevation dependency of the surface climate change signal: a model study. *J Clim* 10:288–296. [https://doi.org/10.1175/1520-0442\(1997\)010%3c0288:edotsc%3e2.0.co;2](https://doi.org/10.1175/1520-0442(1997)010%3c0288:edotsc%3e2.0.co;2)
- Goovaerts P (2000) Geostatistical approaches for incorporating elevation into the spatial interpolation of rainfall. *J Hydrol* 228:113–129. [https://doi.org/10.1016/S0022-1694\(00\)00144-X](https://doi.org/10.1016/S0022-1694(00)00144-X)
- Guo JP, Zhai PM, Wu L, Cribb M, Li ZQ, Ma ZY, Wang F, Chu D, Wang PX, Zhang JH (2014) Diurnal variation and the influential factors of precipitation from surface and satellite measurements in Tibet. *Int J Clim* 34:2940–2956. <https://doi.org/10.1002/joc.3886>
- Guo X, Wang L, Tian L (2016) Spatio-temporal variability of vertical gradients of major meteorological observations around the Tibetan Plateau. *Int J Clim* 36:1901–1916. <https://doi.org/10.1002/joc.4468>
- Hitchens NM, Brooks HE, Schumacher RS (2013) Spatial and temporal characteristics of heavy hourly rainfall in the United States. *Mon Wea Rev* 141:4564–4575. <https://doi.org/10.1175/MWR-D-12-00297.1>
- Houze RA (2012) Orographic effects on precipitating clouds. *Rev Geophys* 50:RG1001. <https://doi.org/10.1029/2011RG000365>
- Huang HL, Wang CC, Chen GTJ, Carbone RE (2010) The role of diurnal solenoidal circulation on propagating rainfall episodes near the eastern Tibetan Plateau. *Mon Wea Rev* 138:2975–2989. <https://doi.org/10.1175/2010MWR3225.1>
- Iwasaki H (2012) Recent positive trend in heavy rainfall in eastern Japan and its relation with variations in atmospheric moisture. *Int J Clim* 32:364–374. <https://doi.org/10.1002/joc.2269>
- Iwasaki H (2015) Increasing trends in heavy rain during the warm season in eastern Japan and its relation to moisture variation and topographic convergence. *Int J Clim* 35:2154–2163. <https://doi.org/10.1002/joc.4115>
- Jiang QF, Smith RB (2003) Cloud timescales and orographic precipitation. *J Atmos Sci* 60:1543–1559. <https://doi.org/10.1175/2995.1>
- Jin X, Wu TW, Li L (2013) The quasi-stationary feature of nocturnal precipitation in the Sichuan Basin and the role of the Tibetan Plateau. *Clim Dyn* 41:977–994. <https://doi.org/10.1007/s00382-012-1521-y>
- Johansson B, Chen D (2003) The influence of wind and topography on precipitation distribution in Sweden: statistical analysis and modelling. *J Clim* 23:1523–1535. <https://doi.org/10.1002/joc.951>
- Kang YZ, Peng XD, Wang SG, Hu YL, Shang KZ, Lu S (2019) Observational analyses of topographic effects on convective systems in an extreme rainfall event in Northern China. *Atmos Res* 229:127–144. <https://doi.org/10.1016/j.atmosres.2019.05.024>
- Kirshbaum DJ (2011) Cloud-resolving simulations of deep convection over a heated mountain. *J Atmos Sci* 68:361–378. <https://doi.org/10.1175/2010JAS3642.1>
- Kirshbaum D, Adler B, Kalthoff N, Christian B, Stefano S (2018) Moist orographic convection: Physical mechanisms and links to surface-exchange processes. *Atmosphere* 9:80. <https://doi.org/10.3390/atmos9030080>
- Leahy PG, Kiely G (2011) Short duration rainfall extremes in Ireland: influence of climatic variability. *Water Res Manage* 25:987–1003. <https://doi.org/10.1007/s11269-010-9737-2>
- Lee KO, Shimizu SG, Maki M, You CH, Uyeda H, Lee D (2010) Enhancement mechanism of the 30 June 2006 precipitation system observed over the northwestern slope of Mt. Halla, Jeju Island, Korea. *Atmos Res* 97:343–358. <https://doi.org/10.1016/j.atmosres.2010.04.008>
- Li J (2017) Hourly station-based precipitation characteristics over the Tibetan Plateau. *Int J Clim* 38:1560–1578. <https://doi.org/10.1002/joc.5281>
- Li J, Chen TR, Li NN (2017) Diurnal variation of summer precipitation across the central Tian Shan Mountains. *J App Mete Clim* 56:1537–1550. <https://doi.org/10.1175/JAMC-D-16-0265.1>
- Li LL, Li J, Chen HM, Yu RC (2019) Diurnal variations of summer precipitation over the Qilian mountains in Northwest China. *J Meteor Res* 33:18–30. <https://doi.org/10.1007/s13351-019-8103-4>
- Li LL, Li J, Yu RC (2020a) Characteristics of summer regional rainfall events over Ili River Valley in Northwest China. *Atmos Res* 243:104996. <https://doi.org/10.1016/j.atmosres.2020.104996>
- Li J, Li YQ, Zhao TL, Reinhard S, Mark M, Jiang XW (2020b) Northeastward propagation of nocturnal precipitation over the Sichuan Basin. *Int J Clim* 1–17. <https://doi.org/10.1002/joc.6886>
- Liang P, Ding Y (2017) The long-term variation of extreme heavy precipitation and its link to urbanization effects in Shanghai during 1916–2014. *Adv Atmos Sci* 34:321–334. <https://doi.org/10.1007/s00376-016-6120-0>
- Liang XZ, Li L, Dai A, Kunkel KE (2004) Regional climate model simulation of summer precipitation diurnal cycle over the United States. *Geophys Res Lett* 31:L24208. <https://doi.org/10.1029/2004GL021054>
- Liao F, Hong YC, Zheng GG (2007) Review of orographic influences on surface precipitation (in Chinese). *Meteor Sci Technol* 35:309–316. <https://doi.org/10.19517/j.1671-6345.2007.03.001>
- Liu D, Zhang YP, Chen GC, Liu Y (2012) Chongqing Weather Forecast Technical Manual (in Chinese). China Meteorological Press, Beijing, p 13
- Liu JF, Chen RS, Qin WW, Yang Y (2011) Study on the vertical distribution of precipitation in mountainous regions using TRMM data (in Chinese). *Adv Water Sci* 22(4):447–454. <https://doi.org/10.1007/s11589-011-0776-4>
- Liu XD, Bai AJ, Liu CH (2009) Diurnal variations of summertime precipitation over the Tibetan Plateau in relation to orographically-induced regional circulations. *Environ Res Lett* 4:940–941. <https://doi.org/10.1088/1748-9326/4/4/045203>
- Luo YL, Wu MW, Ren FM, Li J, Wong WK (2016) Synoptic situations of extreme hourly precipitation over China. *J Clim* 29:8703–8719. <https://doi.org/10.1175/JCLI-D-16-0057.1>
- Peng NZ, Fu BP, Yu Q, Chen M (1995) Some climatologically statistical features of storm with orography in China (in Chinese). *Sci Meteor Sinica* 15:288–292
- Purnell DJ, Kirshbaum DJ (2018) Synoptic control over orographic precipitation distributions during the Olympics Mountains Experiment (OLYMPEX). *Mon Wea Rev* 146:1023–1044. <https://doi.org/10.1175/mwr-d-17-0267.1>
- Qian TT, Zhao P, Zhang FQ, Bao XH (2015) Rainy-season precipitation over the Sichuan Basin and adjacent regions in southwestern China. *Mon Wea Rev* 143:383–394. <https://doi.org/10.1175/MWR-D-13-00158.1>
- Roe GH (2005) Orographic precipitation. *Annu Rev Earth Planet Sci* 33:645–671. <https://doi.org/10.1146/annurev.earth.33.092203.122541>

- Rotunno R, Houze RA (2007) Lessons on orographic precipitation from the Mesoscale Alpine Programme. *Quart J Roy Meteor Soc* 133:811–830. <https://doi.org/10.1002/qj.67>
- Sarmadi F, Huang Y, Thompson G, Steven TS, Michael JM (2019) Simulations of orographic precipitation in the Snowy Mountains of Southeastern Australia. *Atmos Res* 219:183–199. <https://doi.org/10.1016/j.atmosres.2019.01.002>
- Silverman NL, Maneta MP, Chen SH, Harper JT (2013) Dynamically downscaled winter precipitation over complex terrain of the Central Rockies of Western Montana, USA. *Water Resour Res* 49:458–470. <https://doi.org/10.1029/2012wr012874>
- Smith RB (1979) The influence of mountains on the atmosphere. *Adv Geophys* 21:87–230. [https://doi.org/10.1016/S0065-2687\(08\)60262-9](https://doi.org/10.1016/S0065-2687(08)60262-9)
- Smith RB, Barstad I (2004) A linear theory of orographic precipitation. *J Atmos Sci* 61:1377–1391. [https://doi.org/10.1175/1520-0469\(2004\)061%3c1377:altoop%3e2.0.co;2](https://doi.org/10.1175/1520-0469(2004)061%3c1377:altoop%3e2.0.co;2)
- Sokol Z, Bližňák V (2009) Areal distribution and precipitation-altitude relationship of heavy short-term precipitation in the Czech Republic in the warm part of the year. *Atmos Res* 94:652–662. <https://doi.org/10.1016/j.atmosres.2009.03.001>
- Sun JH, Zhang FQ (2012) Impacts of mountain-plains solenoid on diurnal variations of rainfalls along the Mei-Yu front over the East China Plains. *Mon Wea Rev* 140:379–397. <https://doi.org/10.1175/MWR-D-11-00041.1>
- Stevenson SN, Schumacher RS (2014) A 10-year survey of extreme rainfall events in the central and eastern United States using gridded multisensor precipitation analyses. *Mon Wea Rev* 142:3147–3162. <https://doi.org/10.1175/MWR-D-13-00345.1>
- Tao SY (1980) Heavy rain in China (in Chinese). Science Press, Beijing, p 225
- Wang D, Miao JF, Tan ZM (2013) Impacts of topography and land cover change on thunderstorm over the Huangshan (Yellow Mountain) area of China. *Nat Hazards* 67:675–699. <https://doi.org/10.1007/s11069-013-0595-0>
- Wang QW, Xue M, Tan ZM (2016) Convective initiation by topographically induced convergence forcing over the Dabie Mountains on 24 June 2010. *Adv Atmos Sci* 33:1120–1136. <https://doi.org/10.1007/s00376-016-6024-z>
- Wang Z, Yang S, Lau NC, Duan A (2018) Teleconnection between summer NAO and East China rainfall variations: a bridge effect of the Tibetan Plateau. *J Clim*. <https://doi.org/10.1175/jcli-d-17-0413.1>
- Weisse AK, Bois P (2001) Topographic effects on statistical characteristics of heavy rainfall and mapping in the French Alps. *J Appl Meteor* 40:720–740. [https://doi.org/10.1175/1520-0450\(2001\)040%3c0720:TEOSCO%3e2.0.CO;2](https://doi.org/10.1175/1520-0450(2001)040%3c0720:TEOSCO%3e2.0.CO;2)
- White AB, Paul JN (2015) The impacts of California's San Francisco Bay area gap on precipitation observed in the Sierra Nevada during HMT and CalWater. *J Hydro Meteor* 16:1048–1069. <https://doi.org/10.1175/JHM-D-14-0160.1>
- Xu WX, Zipser EJ (2011) Diurnal variations of precipitation, deep convection, and lightning over and east of the eastern Tibetan Plateau. *J Clim* 24(2):448–465. <https://doi.org/10.1175/2010JCLI3719.1>
- Xue M, Luo X, Zhu KF, Sun ZQ, Fei JF (2018) The controlling role of boundary layer inertial oscillations in Meiyu frontal precipitation and its diurnal cycles over China. *J Geo Res* 123(10):5090–5115. <https://doi.org/10.1029/2018jd028368>
- Yu H, Wang L, Yang R, Yang ML, Gao R (2018) Temporal and spatial variation of precipitation in the Hengduan Mountains region in China and its relationship with elevation and latitude. *Atmos Res* 213:1–16. <https://doi.org/10.1016/j.atmosres.2018.05.025>
- Yu RC, Xu YP, Zhou TJ, Li J (2007a) Relation between rainfall duration and diurnal variation in the warm season precipitation over central eastern China. *Geophys Res Lett* 34:L13703. <https://doi.org/10.1029/2007GL030315>
- Yu RC, Zhou TJ, Xiong AY, Zhu YJ, Li JM (2007b) Diurnal variation of summer precipitation over contiguous China. *Geophys Res Lett* 34:L01704. <https://doi.org/10.1029/2006GL028129>
- Yu RC, Li J, Chen HM, Yuan WH (2014) Progress in studies of the precipitation diurnal variation over contiguous China. *J Meteor Res* 28:877–902. <https://doi.org/10.1007/s13351-014-3272-7>
- Yu RC, Yuan WH, Li J (2013) The asymmetry of rainfall process. *China Sci Bull* 58:1850–1856. <https://doi.org/10.1007/s11434-012-5653-6>
- Yuan WH, Yu RC, Fu YF (2014) Study of different diurnal variations of summer long-duration rainfall between the southern and northern parts of the Huai River. *Chin J Geophys* 57:145–153. <https://doi.org/10.1002/cjg2.20092>
- Zhang F, Li G, Yue J (2019a) The moisture sources and transport processes for a sudden rainstorm associated with double low-level jets in the northeast Sichuan Basin of China. *Atmosphere* 10:160. <https://doi.org/10.3390/atmos10030160>
- Zhang YC, Zhang FQ, Sun JH (2014a) Comparison of the diurnal variations of warm-season precipitation for East Asia vs. North America downstream of the Tibetan Plateau vs. the Rocky Mountains. *Atmos Chem Phys* 14:10741–10759. <https://doi.org/10.5194/acp-14-10741-2014>
- Zhang YC, Sun JH, Fu SM (2014b) Impacts of diurnal variation of mountain-plain solenoid circulations on precipitation and vortices east of the Tibetan Plateau during the Meiyu season. *Adv Atmos Sci* 31:139–153. <https://doi.org/10.1007/s00703-016-0484-7>
- Zheng YG, Xue M, Li B, Chen J, Tao ZY (2016) Spatial characteristics of extreme rainfall over China with hourly through 24-hour accumulation periods based on national-level hourly rain gauge data. *Adv Atmos Sci* 33:1218–1232. <https://doi.org/10.1007/s00376-016-6128-5>
- Zhang YH, Xue M, Zhu KF, Zhou BW (2019b) What is the main cause of diurnal variation and nocturnal peak of summer precipitation in Sichuan Basin, China? The key role of boundary layer low-level jet inertial oscillations. *J Geo Res* 124:2643–2664. <https://doi.org/10.1029/2018JD029834>
- Zhou TJ, Yu RC, Chen HM, Dai AG, Pan Y (2008) Summer precipitation frequency, intensity, and diurnal cycle over China: A comparison of satellite data with rain gauge observations. *J Clim* 21:3997–4010. <https://doi.org/10.1175/2008JCLI2028SI>

Publisher's note Springer Nature remains neutral with regard to jurisdictional claims in published maps and institutional affiliations.